NPS ARCHIVE
1958
HAYES, J.

FLUX DISTRIBUTION IN A UNIT CELL OF A URANIUM GRAPHITE SUBCRITICAL ASSEMBLY

JAMES THOMAS HAYES

DUDLEY KNOX LIBRARY
NAVAL POSTGRADUATE SCHOOL
MONTEREY CA 93943-5101

FLUX DISTRIBUTION IN A UNIT CELL OF A URANIUM GRAPHITE SUBCRITICAL ASSEMBLY

by

James Thomas Hayes

A Thesis Submitted to the
Graduate Faculty in Partial Fulfillment of
The Requirements for the Degree of
MASTER OF SCIENCE

Major Subject: Nuclear Engineering

TABLE OF CONTENTS

Page

I. INTRODUCTION 1

II. REVIEW OF THE LITERATURE 3

III. THEORETICAL FLUX DISTRIBUTION IN A SUBCRITICAL ASSEMBLY 5b

IV. THEORETICAL FLUX DISTRIBUTION IN THE UNIT CELL 8

- A. Two Region System 8
- B. Multiregion System 10

V. EXPERIMENTAL EQUIPMENT 14

- A. Subcritical Assembly 14
- B. Unit Cell 20
- C. Counting Equipment 24

VI. EXPERIMENTAL PROCEDURE 25

- A. Determination of γ 25
- B. Correction Factors for Unit Cell Foil Positions 28
- C. Description of Runs in Unit Cell 35
- D. Horizontal Surveys 39

VII. RESULTS 40

- A. Effect of Foil Spacing 40
- B. Effect of Foil Orientation 58
- C. Effect of Foil Size 58
- D. Variation of Flux Along Different Radials 63
- E. Effect of Coolant 77
- F. Cadmium Ratio 90
- G. Comparison of Flux in Unit Cell with Overall Flux in the Assembly 90

TABLE OF CONTENTS (Continued)

Page

VIII. DISCUSSION OF RESULTS 94

A. Techniques for Measuring Flux Distribution in a Unit Cell 94
B. The Flux Distribution in a Unit Cell 96
C. Comparison of Experimental Results with Theory 101

IX. CONCLUSIONS 105

X. SUGGESTIONS FOR FURTHER STUDY 106

XI. LITERATURE CITED 108

XII. ACKNOWLEDGMENTS 110

XIII. APPENDIX 111

I. INTRODUCTION

In homogeneous reactor theory the thermal neutron flux distribution in a given direction in the reactor core is represented as a smooth curve having a shape which is dependent upon the core geometry. In a bare rectangular parallelepiped reactor the flux distribution along each coordinate axis is a cosine curve across the core. In a heterogeneous reactor consisting of rods of fuel regularly arranged in a moderating medium, the general shape of the flux distribution across the core is similar to the cosine distribution of the homogeneous reactor. However, the absorption of neutrons is much higher in the uranium fuel rods than it is in the moderating material, and hence there are local depressions in the neutron flux near the uranium fuel rods.

The theory of the natural uranium heterogeneous reactor has been broken down into microscopic theory and macroscopic theory. Macroscopic theory deals with the overall flux distribution in the reactor and permits the determination of such parameters as critical size and critical mass for a given reactor design. Microscopic theory deals with the local flux distribution in the unit cell of the reactor core, and it permits the calculation of the various lattice

constants, such as thermal utilization, resonance escape probability, lattice diffusion length and material buckling. The subcritical assembly can be used to determine experimentally these lattice constants for a proposed reactor design. Since reactor theory is subject to many limitations and approximations, the subcritical assembly is a valuable tool which can be used to either check or supplement theoretical calculations.

The purpose of this thesis was to investigate the flux distribution in the unit cell of the Iowa State College uranium graphite subcritical assembly. Several techniques for flux measurement using the foil activation method were also investigated. The flux distribution was measured in three different directions inside the unit cell both with and without coolant, and the experimental results were compared with the theoretical flux distribution in the unit cell.

II. REVIEW OF THE LITERATURE

The use of the activation method for measuring thermal neutron flux was covered in detail by Feld (4). Cohen (3) described further use of the activation method and how it could be used to determine the microscopic flux distribution within a unit cell. He also pointed out the particular value of the foil activation method in determining flux distribution near the boundary of two dissimilar mediums where diffusion theory cannot be applied with accuracy. Hummel and Hamermesh (9) investigated the neutron flux depression in the neighborhood of a silver foil but no quantitative results were given for indium foil. Clayton (2) and Richey (11) discussed in detail the foil placement in the unit cell of a uranium graphite lattice and the procedures and corrections used in counting.

Murray (10) developed the flux distribution for a two-region fuel-moderator lattice system based on diffusion theory for monoenergetic neutrons. He further presented a method of estimating the effect of extra absorption due to the presence of other components in the unit cell, such as cladding, tubing, coolant and insulation. In this method it was assumed that all the other components act as poisons which can be tolerated, and hence they do not appreciably disturb

the basic flux distribution in a cell containing only fuel and moderator. Murray's simplified method could be used to determine the thermal utilization in a unit cell but could not be used to determine the point to point flux distribution in the various cell components.

A development of the theoretical flux distribution in the unit cell of a uranium graphite lattice with air coolant was presented by Guggenheim and Pryce (7). Their theory provided for the determination of the flux distribution in the various cell components which included an aluminum clad uranium slug, an air annulus and a graphite moderator. Rumsey and Volkoff (12), in Gast (5), extended the theory to include the moderating effect of a coolant annulus filled with water. Jogenson (8) calculated the physical constants for the subcritical assembly which is the subject of this thesis and determined the effect of coolant and lattice size upon the material buckling.

List of Symbols

Symbol	Units	Meaning
A		Competitive absorption (see p. 11)
A_∞	c/m	Saturation activity
A_{11}	c/m	Corrected saturation activity due to first mode only
A_o	c/m	Corrected saturation activity referred to the center of the unit cell
a	in, cm	Extrapolated width along x-axis
B_{ij}		Blocking term (see p. 12)
B_m^2	in^{-2}, cm^{-2}	Material buckling
b	in, cm	Extrapolated width along y-axis
C_e		End correction term
C_h		Harmonic correction term
c	in, cm	Extrapolated height along z-axis
D	in, cm	Diffusion coefficient
F		Disadvantage factor of uranium, $\frac{\phi(r_u)}{\bar{\phi}_u}$
F'		Overall correction factor (see p. 33)
f		Thermal utilization
f_e		End correction factor
f_h		Harmonic correction factor
f_x		Horizontal position correction factor (see p. 33)
f_z		Vertical position correction factor (see p. 33)
K	neutrons/sec cm^2	Constant which relates flux level to neutron source strength (see p. 7)
K_1		Constant of proportionality
Q	neutrons/sec cm^3	Neutron source term, $\frac{K_1 S}{abD}$
q	neutrons/sec cm^3	Slowing down density
R_i		Relative absorption term (see p. 11)
r	in, cm	Radial distance
S	neutrons/sec	Source strength
S_i		Excess absorption term (see p. 12)
S_u	neutrons/sec cm^3	Source term for uranium
S_m	neutrons/sec cm^3	Source term for moderator

Symbol	Units	Meaning
t	in, cm	Thickness
V	in^3, cm^3	Volume
X		Disadvantage factor of moderator, $\frac{\bar{\phi}_m}{\bar{\phi}_u}$
γ	in^{-1}, cm^{-1}	Inverse relaxation length
δ		Water moderation correction term (see p. 13)
ϕ	neutrons/sec cm^2	Thermal neutron flux
κ	in^{-1}, cm^{-1}	Inverse diffusion length
Σ	in^{-1}, cm^{-1}	Macroscopic absorption cross section

List of Subscripts

Subscript	Meaning
al	aluminum cladding
i	ith medium
j	jth medium
g	graphite
m	moderator
p	process tube
u	uranium
w	water

III. THEORETICAL FLUX DISTRIBUTION IN A SUBCRITICAL ASSEMBLY

The thermal neutron flux in a fairly large subcritical assembly in the central region away from the boundaries and extraneous neutron sources can be represented by (6, p. 281)

$$\nabla^2 \emptyset + B_m^2 \emptyset = 0 \qquad \text{Eq. 1}$$

where $\emptyset$ is the thermal neutron flux, ∇^2 is the Laplacian operator and B_m^2 is the material buckling of the particular lattice system, usually expressed in cm^{-2}. With the usual boundary conditions that the flux is everywhere finite and non-negative and is zero at the extrapolated boundaries the solution to the above equation is

$$\emptyset = \sum_{m=1}^{\infty} \sum_{n=1}^{\infty} \frac{\text{[illegible]}}{\gamma_{mn}} \cos \frac{m\pi x}{a} \cos \frac{n\pi y}{b} \, e^{-\gamma_{mn} z} \cdot \left(1 - e^{-2\gamma_{mn}(c-z)}\right) \qquad \text{Eq. 2}$$

where a, b and c are the extrapolated dimensions of the subcritical assembly in cm and γ_{mn} in cm^{-1} is defined by

$$\gamma_{mn}^2 = \left(\frac{m\pi}{a}\right)^2 + \left(\frac{n\pi}{b}\right)^2 - B_m^2 \qquad \text{Eq. 3}$$

The flux may therefore be represented as

$$\phi = Q \sum_{m=1}^{\infty} \sum_{n=1}^{\infty} \frac{1}{\gamma_{mn}} \cos \frac{m\pi x}{a} \cos \frac{n\pi y}{b} e^{-\gamma_{mn} z} C_e \qquad \text{Eq. 4}$$

where

$$C_e = 1 - e^{-2\gamma_{11}(c-z)}. \qquad \text{Eq. 5}$$

If the expansion is limited to the first and third modes, Equation 4 may be written

$$\phi = Q \frac{e^{-\gamma_{11} z}}{\gamma_{11}} \cos \frac{\pi x}{a} \cos \frac{\pi y}{b} \left[1 + \frac{\gamma_{11} e^{\gamma_{11} z}}{\cos \frac{\pi x}{a} \cos \frac{\pi y}{b}} \left(\frac{e^{-\gamma_{13} z}}{\gamma_{13}} \cos \frac{\pi x}{a} \cos \frac{3\pi y}{b} + \frac{e^{-\gamma_{31} z}}{\gamma_{31}} \cos \frac{3\pi x}{a} \cos \frac{\pi y}{b} + \frac{e^{-\gamma_{33} z}}{\gamma_{33}} \cos \frac{3\pi x}{a} \cos \frac{3\pi y}{b} \right) \right]. \qquad \text{Eq. 6}$$

The harmonic correction term, C_h, is enclosed in the brackets. It may be rearranged as

$$C_h = 1 + \frac{\gamma_{11}}{\gamma_{13}} e^{(\gamma_{11} - \gamma_{13})z} \left(\frac{\cos \frac{3\pi y}{b}}{\cos \frac{\pi y}{b}} + \frac{\cos \frac{3\pi x}{a}}{\cos \frac{\pi x}{a}} \right) + \frac{\gamma_{11}}{\gamma_{33}} e^{(\gamma_{11} - \gamma_{33})z} \left(\frac{\cos \frac{3\pi x}{a} \cos \frac{3\pi y}{b}}{\cos \frac{\pi x}{a} \cos \frac{\pi y}{b}} \right) \qquad \text{Eq. 7}$$

since $\gamma_{13} = \gamma_{31}$ for a square based assembly. The flux may now be written as

$$\phi = K e^{-\gamma_{11} z} \cos \frac{\pi x}{a} \cos \frac{\pi y}{b} C_n C_e \qquad \text{Eq. 8}$$

where $K = \frac{\text{[illegible]}}{\gamma_{11}}$.

From Eq. 3 γ_{mn} is seen to increase rapidly in value for harmonics greater than one since b_m^2 is constant for a given lattice system. Since the quantity $c - z$ is also large for the central region of the assembly, the end correction term, C_e, can be closely approximated by the expression

$$C_e = 1 - e^{-2\gamma_{11}(c - z)}$$

IV. THEORETICAL FLUX DISTRIBUTION IN THE UNIT CELL

A. Two Region System

A first approximation for the thermal neutron flux in the unit cell can be made by use of one group diffusion theory in a two-region fuel-moderator system (10). To simplify the mathematics the square cell is replaced by a cylindrical cell of equal area. The diffusion equation for the fuel is

$$D_u \nabla^2 \phi_u - \phi_u \Sigma_u + S_u = 0 \qquad \text{Eq. 9}$$

and for the moderator is

$$D_m \nabla^2 \phi_m - \phi_m \Sigma_m + S_m = 0 \qquad \text{Eq. 10}$$

where D is the diffusion coefficient in cm, ϕ is the thermal neutron flux in neutrons/cm^2 sec, Σ is the macroscopic absorption cross section in cm^{-1}, and S is the thermal neutron production rate per cm^3. With the assumptions that $S_u = 0$, S_m is constant, ϕ does not vary along the cell axis, and that ϕ is constant at any given cell radius, the solutions to Eqs. (9) (10) are

$$\phi_u (r) = A\, I_0 (\kappa_u r) \qquad \text{Eq. 11}$$

and

$$\phi_m(r) = C\, M_0\,(r\kappa_m) + \frac{S_m}{\Sigma_m} \qquad \text{Eq. 12}$$

respectively, where

$$\frac{A}{S_m} = \frac{D_m \kappa_m M_1(\kappa_m r_u)}{\Delta}\,, \qquad \text{Eq. 13}$$

$$\frac{C}{S_m} = \frac{-D_u \kappa_u I_1(\kappa_u r_u)}{\Delta}\,, \qquad \text{Eq. 14}$$

$$\Delta = \Sigma_m \Big[D_m \kappa_m I_0(\kappa_u r_u) M_1(\kappa_m r_u) + D_u \kappa_u I_1(\kappa_u r_u) M_0(\kappa_m r_u) \Big]\,, \qquad \text{Eq. 15}$$

$$M_0(\kappa_m r) = K_0(\kappa_m r) + \frac{K_1(\kappa_m r_2)}{I_1(\kappa_m r_2)} I_0(\kappa_m r)\,, \qquad \text{Eq. 16}$$

and

$$M_1(\kappa_m r) = K_1(\kappa_m r) - \frac{K_1(\kappa_m r_2)}{I_1(\kappa_m r_2)} I_1(\kappa_m r)\,. \qquad \text{Eq. 17}$$

In the above equations κ is the inverse diffusion length for the given medium and I_0, I_1, K_0 and K_1 are modified Bessel functions of the zero and first order. The physical constants for the subcritical assembly were previously determined (8) and are listed in Table 8 along with the various dimensions of the unit cell. With these constants and a table of Bessel functions (1) the flux in the fuel and in the moderator was determined from Eqs. 11 and 12 assuming

$S_m = 1 \frac{\text{neutron}}{\text{cm}^2 \text{ sec}}$. The theoretical flux distribution normalized to the flux at the cell boundary is shown in Figure 31.

B. Multiregion System

The theoretical flux distribution in a multiregion unit cell consisting of fuel, cladding, water coolant, aluminum process tube and graphite moderator is based on the thermal utilization equation derived by Rumsey and Volkoff (5, 12),

$$f_m = f_o \, (1 + \delta) \qquad \text{Eq. 18}$$

where

$$\frac{1}{f_o} - 1 = R_{al} + R_w + R_p + R_g + S_w + S_g + B_{wp} + B_{wg} \qquad \text{Eq. 19}$$

The subscripts al, w, p, g and u denote aluminum cladding, water, process tube, graphite and uranium respectively. An abbreviated explanation of Eqs. 18 and 19 follows.

Thermal utilization is the ratio of the number of thermal neutrons captured in uranium to the total number of thermal neutrons captured in the lattice. For a two region fuel-moderator system it may be written as

$$f = \frac{\Sigma_u V_u \bar{\emptyset}_u}{\Sigma_u V_u \bar{\emptyset}_u + \Sigma_m V_m \bar{\emptyset}_m} = \frac{1}{1 + \dfrac{\Sigma_m V_m}{\Sigma_u V_u} X} \qquad \text{Eq. 20}$$

where X is the disadvantage factor for the moderator

$$X = \frac{V_m}{V_u} \frac{\kappa_m r_u}{2} \frac{M_0 (\kappa_m r_u)}{M_1 (\kappa_m r_u)} - 1 \qquad \text{Eq. 21}$$

Thermal utilization may also be expressed as

$$f = \frac{1}{1 + A} \qquad \text{Eq. 22}$$

Alternately, the competitive absorption,

$$\frac{1}{f} - 1 = A, \qquad \text{Eq. 23}$$

is the ratio of the number of thermal neutrons captured by the moderator to the number captured by the uranium. The addition of other regions to the lattice can be accommodated by expressing the competitive absorption as

$$\frac{1}{f} - 1 = A_1 + A_2 + A_3 + - - - - - \qquad \text{Eq. 24}$$

where the various A terms now denote the competitive absorption for a given region. The competitive absorption terms for a given region may be further broken down as

$$A_i = R_i + S_i + B_{ij} \qquad \text{Eq. 25}$$

R_i is the "relative absorption" term and denotes the number of thermal neutrons captured in the ith medium per thermal neutron captured in the uranium if the thermal neutron density in the ith medium were uniformly equal to the thermal neutron density at the uranium-aluminum interface.

$$K_i = \frac{\Sigma_i V_i}{\Sigma_u V_u} F \qquad \text{Eq. 26}$$

where V denotes volume and F is the disadvantage factor of the uranium expressed as

$$F = \frac{\phi_u(r_u)}{\overline{\phi}_u} \qquad \text{Eq. 27}$$

S_i is the "excess absorption term" and denotes the excess number of neutrons captured in the ith medium per thermal neutron absorbed in the uranium due to the excess neutron density in the ith medium over the neutron density at the i-jth interface. For the water

$$S_w = \frac{1}{3} \kappa_w^2 t_w^2 \qquad \text{Eq. 28}$$

and for the graphite

$$S_g = X \left[1 + K_{al} + K_p + K_w + B_{wp} + S_w \right] . \qquad \text{Eq. 29}$$

B_{ij} is the "blocking term" and denotes the excess number of thermal neutrons absorbed in the jth medium per thermal neutron absorbed in the uranium due to the neutron density rise across the ith medium.

$$B_{wp} = \kappa_w^2 t_w^2 \frac{\Sigma_p V_p}{\Sigma_w V_w} \qquad \text{Eq. 30}$$

and

$$B_{wg} = \kappa_w^{\,2} t_w^{\,2} \left\{ \frac{\Sigma_g V_g}{\Sigma_w V_w} + F_g \left[\frac{1}{2} + \frac{\Sigma_{a1} V_{a1}}{\Sigma_w V_w} \right] \right\} \qquad \text{Eq. 31}$$

where t_w is the thickness of the water annulus. All competitive absorption terms except those remaining in Eq. 19 are negligible.

The term δ in Eq. 18 accounts for the moderating effect of the water and is expressed as

$$\delta = \frac{\dfrac{q_w V_w}{q_g V_g} \left[X + \dfrac{1}{2} \kappa_w^{\,2} t_w^{\,2} \dfrac{\Sigma_g V_g}{\Sigma_w V_w} \right]}{1 + \dfrac{q_w V_w}{q_g V_g}} \qquad \text{Eq. 32}$$

where q is the production rate of thermal neutrons per unit volume per second. The ratio of q_w/q_g is equal to 20 (11, p. 22).

V. EXPERIMENTAL EQUIPMENT

A. Subcritical Assembly

1. General description

The subcritical assembly used for the experimental investigations is shown in Figure 1. It consisted of fourteen layers of graphite, each containing ten blocks 60 in. long. In the first nine layers the block cross section was 6 in. by 6 in., while in the top five layers the block cross section was 5 in. by 6 in. The top blocks were laid with the 6-in. side horizontal giving the entire assembly the dimensions of 60 in. by 60 in. by 79 in. high. The graphite blocks were cut from 7-in. diameter cylindrical rods so that the rounded corners provided holes in the assembly for the insertion of fuel elements or measuring apparatus.

The assembly was covered on the top and sides by covers made up of a sandwich of masonite, plywood, and a 0.010 in. thick sheet of cadmium. The purpose of the cadmium was to provide a "black boundary" to the neutrons. The assembly was mounted on a base which provided a space underneath about one foot high for the insertion of three water tanks. Two tanks extending the length of the assembly were filled and

Figure 1. The subcritical assembly

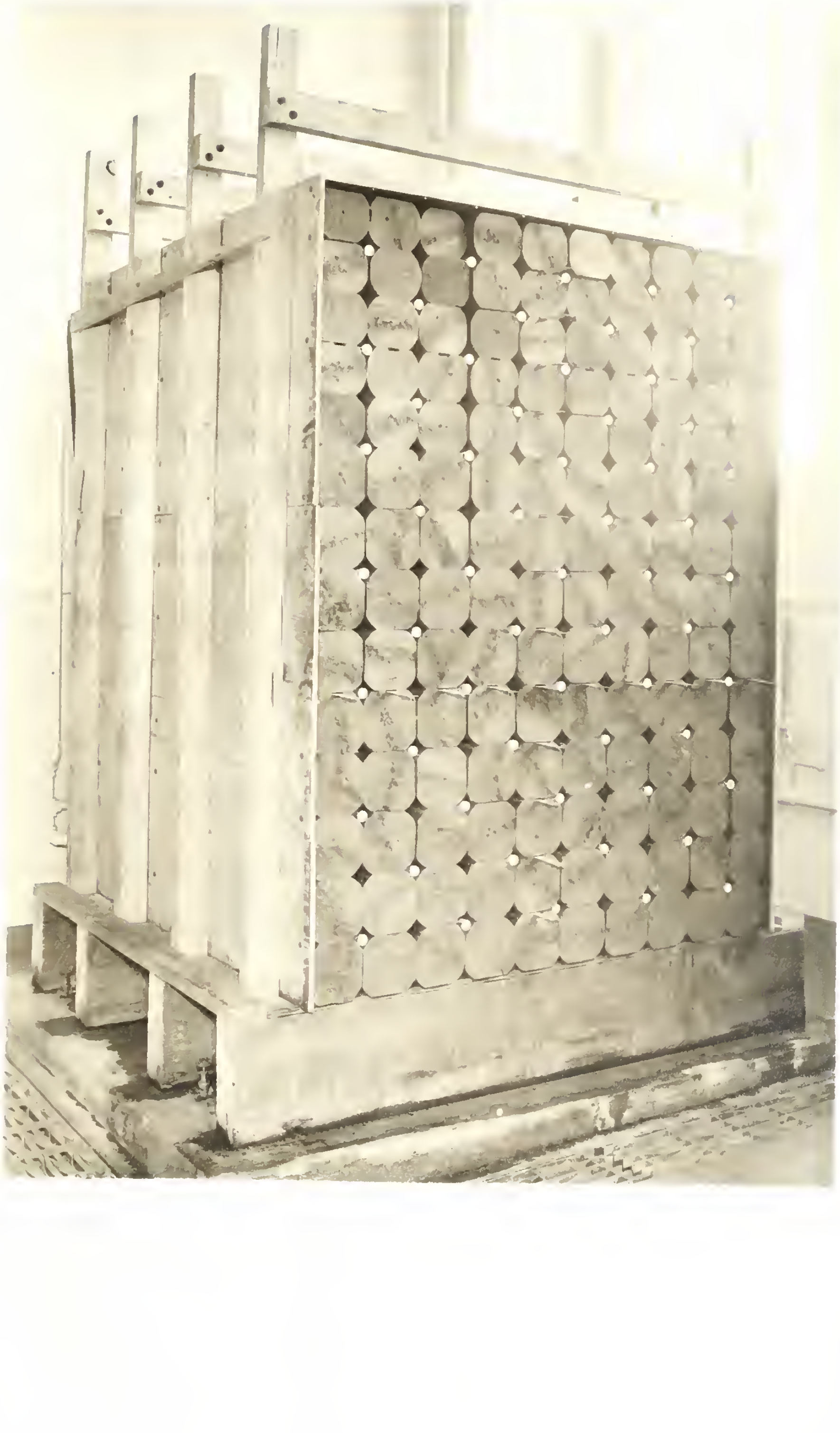

placed on each side of the source. The center tank consisted of three compartments. The two end compartments, each about 26 in. long, were filled with water. The center compartment was left dry, and in it was placed a small table on which the sources were mounted.

2. Sources

The assembly source consisted of five individual plutonium-beryllium neutron sources, each emitting approximately 1.63×10^6 neutrons per second. Each source was contained in a stainless steel and tantalum container which was one inch in diameter and 1 3/8 in. high. When placed on the small source table which was located underneath the center of the assembly the tops of the source containers were about 1/16 in. beneath the floor of the assembly. The five sources were arranged in a cruciform shape oriented on the x and y axes of the coordinate system used as shown in Figure 2.

3. Fuel elements

The assembly was loaded with fuel elements as shown in Figure 1 by filling every other hole giving an 8.48-in. square lattice in the lower region of the assembly. The fuel assembly consisted of canned natural uranium slugs wrapped with 2S aluminum wire spacers and inserted in 61S aluminum process tubes. The uranium fuel itself consisted

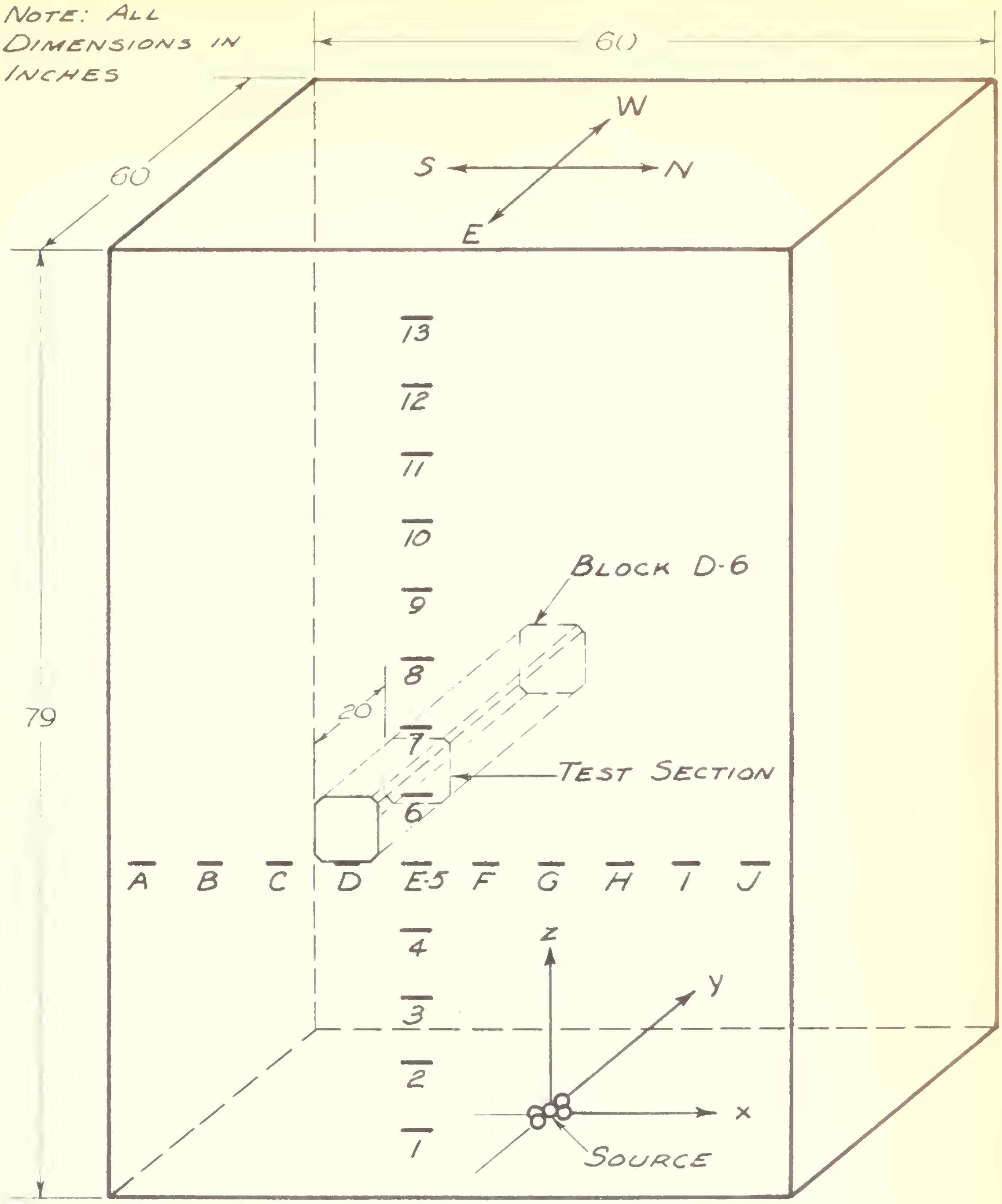

Figure 2. Subcritical assembly

of rods 1 in. in diameter and 8 in. long. The 28 aluminum cans had a 0.040-in. wall thickness and the end caps were 0.200 in. thick. Thus the overall dimensions of the fuel slugs were 8.40 in. long by 1.080 in. in diameter. Seven slugs were inserted in each process tube. The aluminum process tubes were 62 in. long, had an outside diameter of 1.375 in. and a wall thickness of 0.035 in. The effective thickness of the coolant annulus between the slug and process tube was 0.112 in. The aluminum wire spacer was 0.102 in. in diameter, and approximately ten feet of wire was used in each fuel assembly. The ends of the process tubes were plugged with number seven rubber stoppers when making runs with coolant.

4. Indium foil positions

Slots for inserting indium foils were located as shown in Figure 2, and were used in making vertical and horizontal flux surveys of the overall assembly. A grid system was used in identifying blocks and/or foil positions in the assembly. Layers were numbered from bottom to top from 1 to 14 and the ten columns were designated A through J from left to right on the east face of the assembly. The foils normally used for pile surveys were 1.0 inch by 1.5 in. by 0.003 in. thick and weighed approximately 0.6 mg each. These were mounted on aluminum backing and were inserted in the pile by means of an

aluminum strip foil holder. It was thus possible to obtain surveys at x = -3 in., z = 30 in. and at any value of y between zero and -30 in.

D. Unit Cell

Block D-6 was cut vertically at a point 20 in. in from the east face of the assembly to provide a test section at which unit cell flux measurements could be made. This particular position was selected to keep harmonic effects to a minimum. The blocks above block D-6 were supported by a lever arrangement so that one third of block D-6 could easily be moved in and out of the pile. Grooves [illegible] in. deep and 0.015 in. wide were cut into the sawed-off face of the graphite block spaced 3/4 in. apart. The unit cell together with the foil positions is shown in Figure 3. On the P and R radials there were seven foil positions within the fuel assembly numbered from 1 to 7 as shown for the P radial in Figure 3. Since there was no air space between the process tube and the graphite on the Q radial there were only four foil positions, numbered Q1 through Q4, within the fuel assembly on this radial. The foil positions in the graphite were numbered consecutively proceeding out the respective radial as shown in Figure 3. Foil positions along the P and R radials extended to the unit cell boundary while those

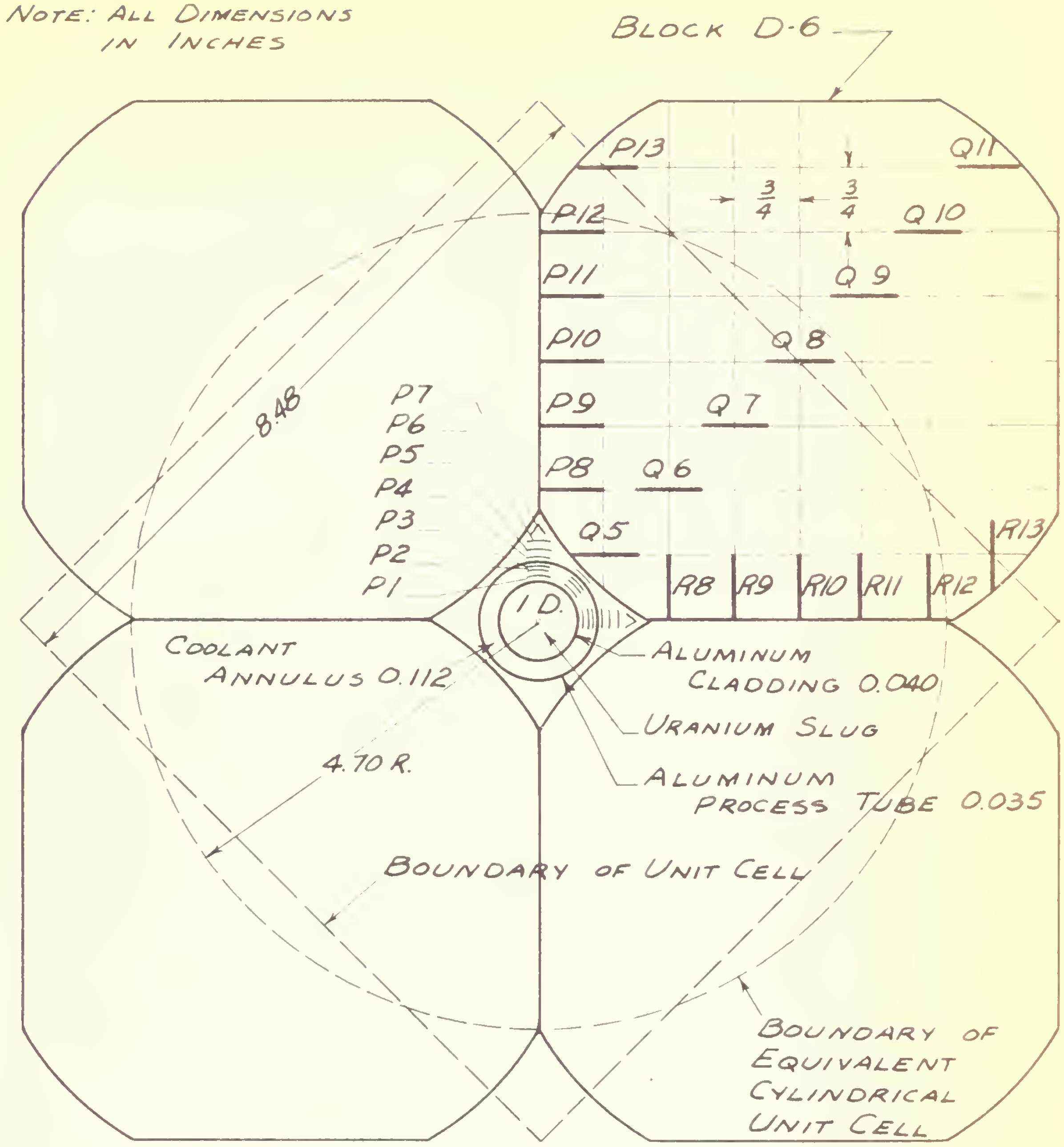

Figure 3. Unit cell

along the Q radial extended to the fuel assembly in the adjacent cell. The coordinates of each foil position are listed in Table 1. A process tube was cut at a point 20 in. in from the east face to permit placing foils inside the coolant annulus of the fuel assembly. On runs made with

Table 1. Unit cell foil positions and position correction factors

Position	x in.	z in.	Radial distance in.	f_x	f_z
0.0	-12.00	30.00	0	1.000	1.000
P1	-12.00	30.54	0.54	1.000	1.034
P2	-12.00	30.60	0.60	1.000	1.043
P3	-12.00	30.65	0.65	1.000	1.052
P4	-12.00	30.69	0.69	1.000	1.052
P5	-12.00	30.75	0.75	1.000	1.052
P6	-12.00	30.81	0.81	1.000	1.061
P7	-12.00	30.87	0.87	1.000	1.066
P8	-12.00	31.50	1.50	1.000	1.110
P9	-12.00	32.25	2.25	1.000	1.174
P10	-12.00	33.00	3.00	1.000	1.234
P11	-12.00	33.75	3.75	1.000	1.300
P12	-12.00	34.50	4.50	1.000	1.360
P13	-12.00	35.25	5.25	1.000	1.440
Q1	-11.62	30.38	0.54	0.985	1.026
Q2	-11.58	30.42	0.60	0.985	1.030
Q3	-11.54	30.46	0.65	0.985	1.030
Q4	-11.51	30.49	0.69	0.982	1.034
Q5	-11.25	30.75	1.06	0.974	1.057
Q6	-10.50	31.50	2.12	0.952	1.110
Q7	- 9.75	32.25	3.18	0.931	1.174
Q8	- 9.00	33.00	4.24	0.913	1.234
Q9	- 8.25	33.75	5.30	0.898	1.300
Q10	- 7.50	34.50	6.36	0.882	1.360

Table 1. (Continued)

Position	x in.	z in.	Radial distance in.	f_x	f_z
Q11	- 6.75	35.25	7.42	0.870	1.440
R1	-11.46	30.0	0.54	0.980	1.000
R2	-11.40	30.0	0.60	0.979	1.000
R3	-11.35	30.0	0.65	0.975	1.000
R4	-11.31	30.0	0.69	0.975	1.000
R5	-11.25	30.0	0.75	0.972	1.000
R6	-11.19	30.0	0.81	0.971	1.000
R7	-11.13	30.0	0.87	0.968	1.000
R8	-10.50	30.0	1.50	0.952	1.000
R9	- 9.75	30.0	2.25	0.931	1.000
R10	- 9.00	30.0	3.00	0.913	1.000
R11	- 8.25	30.0	3.75	0.898	1.000
R12	- 7.50	30.0	4.50	0.882	1.000
R13	- 6.75	30.00	5.25	0.870	1.000

coolant the process tube was sealed with waterpoof electrician's tape.

Three sizes of indium foil were used for flux measurements in the unit cell as follows:

Table 2. Indium foils used in unit cell

Foil	Size (in.)	Average wt. (mg)
Small	½ x ½	0.096
Medium	½ x 3/4	0.130
Large	½ x 7/8	0.152

The weight of each foil was determined to the nearest tenth of a milligram. The foils were mounted on scotch tape backing and were held in place in positions around the fuel element by means of electrician's tape or adhesive tape. Radial positions 2, 5, 6 and 7 were obtained by bending the tape into an inverted "U" with the foil placed at the desired position.

C. Counting Equipment

A Nuclear-Chicago model 181 A scaler and model D34 mica end window counter were used to count irradiated indium foil activities. The counter was placed inside a 2-in. thick lead shield which resulted in an average background count of 20 counts per minute. An automatic timer which could be set for any desired counting time was used in conjunction with the scaler. The indium foil counting geometry was held constant by means of trays on which the foil positions had been marked.

VI. EXPERIMENTAL PROCEDURE

A. Determination of γ

In order to correct foil readings obtained at various points in the subcritical assembly, it was necessary to determine γ, the inverse relaxation length for the thermal neutron flux in the assembly. Vertical flux surveys were made at $x = -3$ in. and $y = -10$ in. from $z = 18$ in. to $z = 54$ in. Points for z less than 18 in. and greater than 54 in. were not used due to the proximity of the source in the first instance and the change in lattice size in the latter. The indium foils weighing an average of 0.5953 gm were used for these surveys, and they were irradiated for a minimum of eight hours which gave an induced activity of 99.8 per cent of the saturation activity. Observed activities were corrected back to time of removal from the assembly, and this saturation activity was then divided by the particular foil weight to give the normalized saturation activity, A_∞, in counts per minute per gram of indium. Surveys were made with and without water in the coolant annuli. Counting times were adjusted to keep the relative standard deviation of the observed counting rate less than 4 per cent.

The normalized saturation activities were plotted on

semi-logarithmic paper and a straight line was faired through the points. The slope of this line yielded a trial value for γ_{11}, which was now used to compute the harmonic and end correction terms, C_e and C_h. These correction terms were then divided into the normalized saturation activities to give A_{11}, the activities which would be obtained if the 1,1 harmonic of the flux distribution were the only one present. To further refine the value of γ_{11} it was necessary to use an iterative process whereby new correction terms would be computed and applied to the original normalized saturation activities to obtain new corrected values of A_{11}. The method of least squares was applied to obtain a new value for γ_{11}. For the purposes of this investigation sufficient accuracy in the value of γ_{11} was obtained by going through the iterative procedure only once. Harmonic effects beyond the third harmonic were found to be negligible and were ignored in calculating the harmonic correction terms. Similarly the end correction term, C_e, was found to have negligible effect beyond the first harmonic, so that C_e was assumed to be simply $1-e^{-2\gamma_{11}(c-z)}$ where c was taken equal to 79 in., the height of the assembly.

The values of γ_{mn} for the higher harmonics were calculated from the relation (2)

$$\gamma_{mn}^2 = \left(\frac{\pi}{a}\right)^2 (m^2 + n^2 - 2) + \gamma_{11}^2 \qquad \text{Eq. 33}$$

Table 3. Inverse relaxation length and buckling

		Without coolant	With coolant
γ_{11}	(in^{-1})	0.0705	0.0713
$\gamma_{13} = \gamma_{31}$	(in^{-1})	0.1598	0.1600
γ_{33}	(in^{-1})	0.215	0.215
B^2	(in^{-2})	1.8×10^{-4}	0.6×10^{-4}
B^2	(cm^{-2})	28.8×10^{-6}	9.6×10^{-6}

where a is the length of the side of the square-based assembly including the extrapolation distance. The value of a was measured to be 62 in. The values of γ_{mn} for the various harmonics with and without coolant are listed in Table 3 together with the values for the buckling. The material buckling was evaluated from the equation for a square-based assembly,

$$B_m^2 = 2\left(\frac{\pi}{a}\right)^2 - \gamma_{11}^2 \qquad \text{Eq. 34}$$

The values of harmonic and end correction terms, C_e and C_h, the normalized saturation activity, A_∞, and the corrected activity due to the first mode only, A_{11}, are listed in Table 4. The corrected activities, A_{11}, are plotted in Figures 4 and 5.

Table 4. Vertical flux survey at x = -3 in., y = -10 in.

Position	z (in.)	C_e	C_h	C_eC_h	A_∞ (c/m)	A_{11} (c/m)
			Without coolant			
E3	18	0.9997	1.0847	1.0847	2750	2540
E4	24	0.9994	1.0491	1.0491	1943	1854
E5	30	0.9989	1.0285	1.0280	1088	1051
E6	36	0.9974	1.0168	1.013	842	831
E7	42	0.9941	1.0097	1.002	535	534
E8	48	0.9810	1.0057	0.987	339	343
E9	54	0.9680	1.0033	0.972	181	188
			With coolant			
E3	18	0.9998	1.0869	1.0869	2860	2635
E4	24	0.9996	1.0505	1.0505	1862	1772
E5	30	0.9989	1.0296	1.029	1153	1121
E6	36	0.9976	1.0171	1.013	780	770
E7	42	0.9945	1.0100	1.004	503	501
E8	48	0.9870	1.0058	0.994	308	310
E9	54	0.9700	1.0034	0.974	193	198

B. Correction Factors for Unit Cell Foil Positions

Harmonic and end correction factors, f_h and f_e, were calculated for each foil position in the unit cell. It should be noted that the correction factor is equal to the reciprocal of the correction term

$$f_e = \frac{1}{C_e} \quad , \quad f_h = \frac{1}{C_h} \qquad \text{Eq. 35}$$

Harmonic and end correction factors for each foil position in

Figure 4. Vertical flux survey without coolant

The vertical pile survey was made at x = -3 in., y = -10 in. with 1 in. by 1⅛ in. foils. The vertical unit cell survey was made at x = -10 in., y = -10 in. with ½ in. by 3/4 in. foils at spacing 2. Unit cell survey data was normalized to pile survey data.

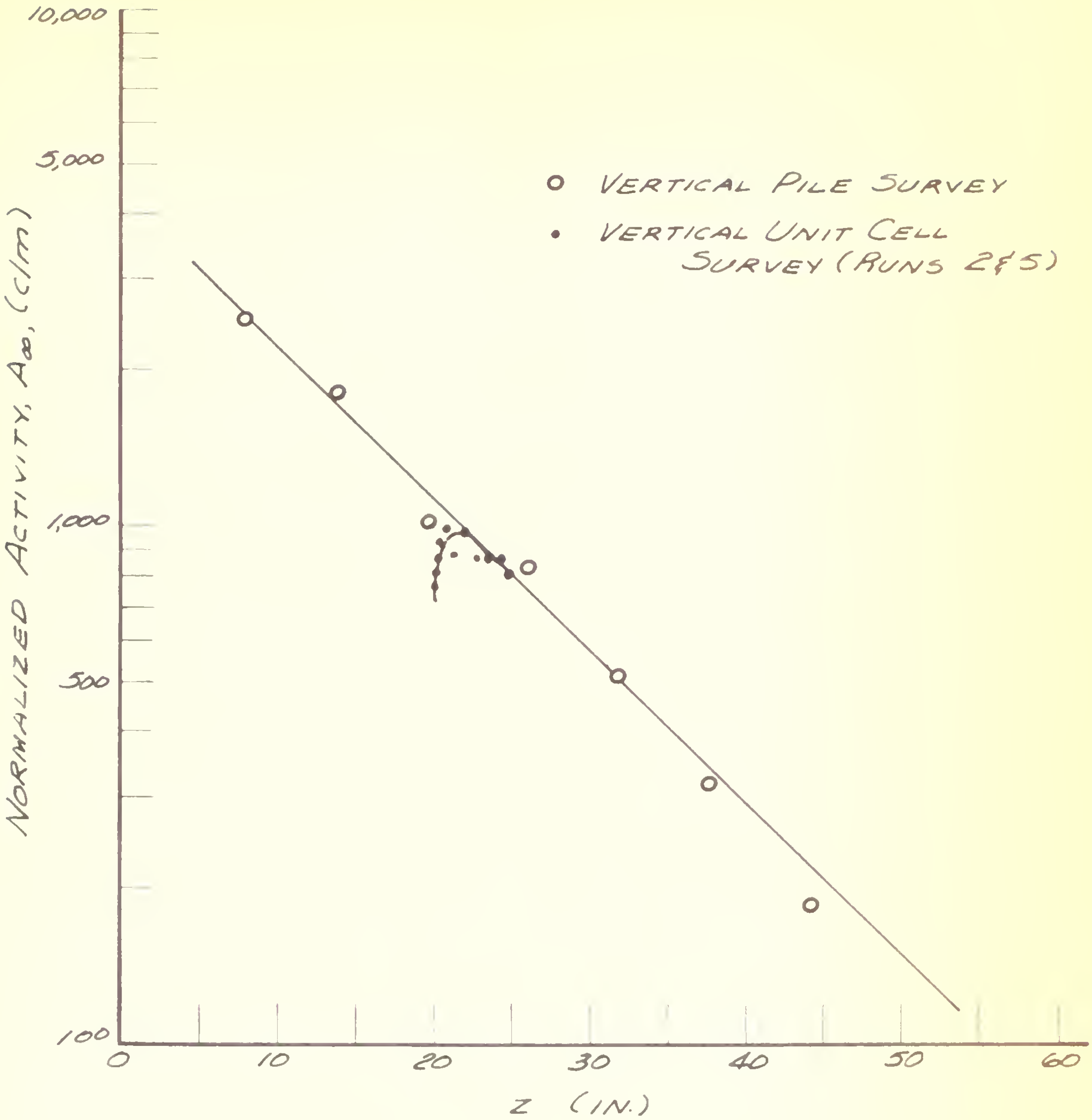
10,000
5,000
1,000
500
100
NORMALIZED ACTIVITY, A_∞, (c/m)
0
10
20
30
40
50
60
Z (IN.)
○ VERTICAL PILE SURVEY
• VERTICAL UNIT CELL SURVEY (RUNS 2 & 5)

Figure 5. Vertical flux survey with water coolant

The vertical pile survey was made at x = -3 in., y = -10 in. with 1 in. by 1½ in. foils. The vertical unit cell survey was made at x = -10 in., y = -10 in. with ½ in. by 3/4 in. foils at spacing 2. Unit cell survey data was normalized to pile survey data.

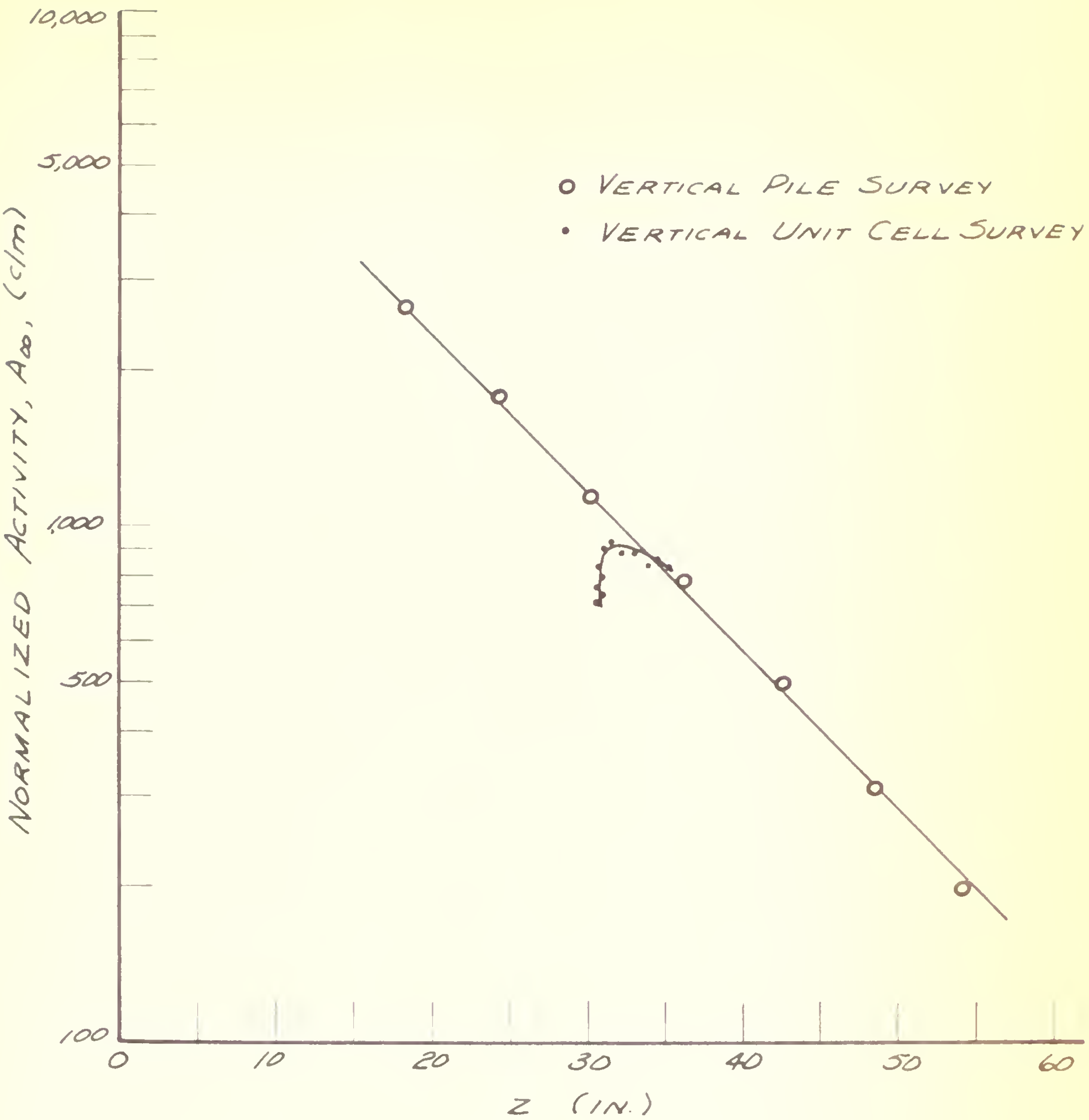
10,000
5,000
1,000
500
100
NORMALIZED ACTIVITY, A_∞, (c/m)
o VERTICAL PILE SURVEY
• VERTICAL UNIT CELL SURVEY
0
10
20
30
40
50
60
Z (IN.)

the unit cell are listed in Table 5.

In order to compare the flux distribution in the unit cell with the theoretical flux distribution it was necessary to convert the activities at the various foil positions to a common reference point. The point chosen was the center of the unit cell examined which corresponded to the center of the uranium slug at x = -12 in., z = 30 in. It was therefore necessary to make corrections to all activities for the cosine distribution in the x direction and for the exponential decrease in the z direction. These position corrections were called f_x and f_z respectively, and they were evaluated from the equations

$$f_x = \frac{\left[\cos \frac{\pi x}{a}\right]_{x=-12}}{\left[\cos \frac{\pi x}{a}\right]_{x=x}} = \frac{\cos\left(\frac{12\pi}{62}\right)}{\cos\left(\frac{\pi x}{62}\right)} \qquad \text{Eq. 36}$$

$$f_z = e^{-\gamma(30-z)} \qquad \text{Eq. 37}$$

The above factors were multiplied together to give one overall correction factor, F, for each position in the unit cell as follows

$$F' = f_x \, f_z \, f_e \, f_h \qquad \text{Eq. 38}$$

Values of the position correction factors are listed in Table 1, and values of F′ are listed in Table 5.

Table 5. Unit cell end and harmonic correction factors

Position	f_e	With coolant		Without coolant	
		f_h	F'	f_h	F'
0.0	1.001	1.008	1.010	1.009	1.010
P1	1.002	1.008	1.046	1.009	1.042
P2	1.002	1.008	1.046	1.008	1.052
P3	1.002	1.008	1.055	1.008	1.061
P4	1.002	1.008	1.060	1.008	1.061
P5	1.002	1.008	1.060	1.008	1.061
P6	1.002	1.008	1.073	1.007	1.068
P7	1.002	1.008	1.073	1.007	1.072
P8	1.002	1.008	1.123	1.006	1.116
P9	1.002	1.007	1.190	1.006	1.122
P10	1.002	1.007	1.251	1.006	1.240
P11	1.002	1.007	1.320	1.005	1.307
P12	1.002	1.005	1.381	1.005	1.368
P13	1.002	1.005	1.468	1.004	1.448
Q1	1.002	1.005	1.019	1.007	1.017
Q2	1.002	1.005	1.019	1.006	1.020
Q3	1.002	1.005	1.019	1.004	1.021
Q4	1.002	1.004	1.022	1.004	1.021
Q5	1.002	1.002	1.031	1.003	1.032
Q6	1.002	0.999	1.062	0.999	1.057
Q7	1.002	0.995	1.100	0.995	1.090
Q8	1.002	0.994	1.128	0.992	1.107
Q9	1.002	0.992	1.170	0.990	1.157
Q10	1.002	0.990	1.200	0.989	1.188
Q11	1.002	0.988	1.270	0.989	1.241
R1	1.001	1.008	0.988	1.005	0.985
R2	1.001	1.008	0.987	1.004	0.984
R3	1.001	1.007	0.982	1.004	0.980
R4	1.001	1.006	0.981	1.004	0.980
R5	1.001	1.004	0.978	1.003	0.976
R6	1.001	1.003	0.975	1.003	0.975
R7	1.001	1.003	0.972	1.002	0.970
R8	1.001	1.000	0.952	1.000	0.952
R9	1.001	0.997	0.929	0.995	0.926
R10	1.001	0.994	0.907	0.992	0.905

Table 5. (Continued)

Position	f_e	With coolant		Without coolant	
		f_h	F'	f_h	F'
R11	1.001	0.989	0.888	0.988	0.887
R12	1.001	0.986	0.870	0.985	0.869
R13	1.001	0.984	0.855	0.982	0.854

C. Description of Runs in Unit Cell

In investigating the flux in the unit cell runs were made along the P, Q and R radials emanating from the center of the fuel assembly as shown in Figure 3. Runs 1 through 16 were made with no water in the coolant annulus and will hereafter be called "dry" runs. Runs 17 through 32 were made with water in the coolant annulus and will hereafter be called "wet" runs. The medium sized foils were used on all the dry runs, whereas on the wet runs the foil size was varied to study the effect of this parameter on the induced activities. The foil spacing was varied on the dry runs but was held constant on the wet runs.

"Spacing 1" is defined as that spacing along a radial when all the foil positions in the graphite were filled for a run. "Spacing 2" corresponded to a foil being placed in every other foil position, and "spacing 3" corresponded to a foil being placed in every third foil position along a given

radial. The above spacing refers only to those foils placed in the graphite block. Foils were placed in positions in the fuel assembly two at a time while the foils in the graphite were being irradiated, and this was called "normal spacing" for foils in the fuel assembly. Thus, the data for runs 5, 11 and 16 were actually taken during runs 1, 2, 3, 6, 7, 8, 10, 12, 13 and 14. The fuel assembly foil readings were grouped into individual runs simply for ease of reference. At least one run along each radial was made with all or almost all of the foil positions on that radial filled both in the fuel assembly and in the graphite. These were runs 4, 15, 19, 25 and 30, and the foil spacing in the fuel assembly on these runs was designated as "close-packed". On these runs medium sized indium foils were used.

Foils were normally placed along the P and Q radials in the horizontal position, and along the R radial in the vertical position as indicated in Figure 3. On runs 6, 8 and 10 medium foils were placed with spacing 1 along the Q radial in a horizontal, a vertical and an L-shaped position respectively. The L-shaped position was obtained by bending the foil into a 90° angle and inserting it into the block so that it pointed outward along the radial.

On runs 27 and 32 along the Q and R radials respectively the indium foils were wrapped in 0.010-in. cadmium sheet and irradiated. On these runs only one cadmium wrapped foil was

placed in the block at a time in order to avoid too large a depression in the thermal neutron flux due to the presence of the cadmium.

On all but the initial runs the counting times used were either two or three minutes. It was found that there was excessive scatter in the experimental data using the two minute counts, and therefore three minute counts were adopted for all the later runs. With the three minute counts the maximum relative standard deviation in the counting rate was 5 per cent with the average being 3 to 4 per cent. Exclusive of those runs made with close-packed spacing, the foil loading for each irradiation averaged four foils along the Q radial and eight foils along the P and R radials. Runs were made along the P and R radials simultaneously. For any one irradiation all the foils were counted through once, and then a second count was taken. The average of the two saturation activities thus obtained was used as a measure of the flux. If the foil activities were high enough, a third and even fourth count was made and the average of all saturation activities was used. All runs made in the unit cell are listed in Table 6.

Table 6. List of runs in unit cell

Run no.	Coolant	Radial	Foil size	Foil spacing[a]	Foil orientation
1	None	P	medium	1	horizontal
2	None	P	medium	2	horizontal
3	None	P	medium	3	horizontal
4	None	P	medium	1 CP	horizontal
5	None	P	medium	normal	radial
6	None	Q	medium	1	horizontal
7	None	Q	medium	3	horizontal
8	None	Q	medium	1	vertical
10	None	Q	medium	1	L-shaped
11	None	Q	medium	normal	radial
12	None	R	medium	1	vertical
13	None	R	medium	2	vertical
14	None	R	medium	3	vertical
15	None	R	medium	1 CP	vertical
16	None	R	medium	1	radial
17	Water	P	large	2	horizontal
18	Water	P	medium	2	horizontal
19	Water	P	medium	1 CP	horizontal
20	Water	P	large/medium	normal	radial
21	Water	P	small	normal	radial
22	Water	Q	large	3	horizontal
23	Water	Q	medium	3	horizontal
24	Water	Q	small	3	horizontal
25	Water	Q	medium	1 CP	horizontal
26	Water	Q	large/medium	normal	radial
27	Water	Q	medium		horizontal
28	Water	R	large	2	vertical
29	Water	R	medium	2	vertical
30	Water	R	medium	1 CP	vertical
31	Water	R	large/medium	normal	radial
32	Water	R	medium	2	vertical

[a] CP = close packed

Table 7. Horizontal flux survey at y = -10 in., z = 30 in.

Position	x (in.)	Normalized activity (c/m)	
		Without coolant	With coolant
A5	-27	205	244
B5	-21	400	512
C5	-15	835	847
D5	- 9	1088	1062
E5	- 3	1080	1153
F5	3	1248	1255
G5	9	1092	1165
H5	15	790	809
I5	21	601	567
J5	27	241	268

D. Horizontal Surveys

Horizontal pile surveys were made in the x direction at y = -10 in. and z = 30 in. both with and without water in the coolant annulus to determine whether or not the transverse flux distribution in the subcritical assembly was symmetrical. The normalized activities from these surveys are listed in Table 7 and are plotted in Figure 29.

VII. RESULTS

The raw data for all runs was reduced to normalized saturation activities, A_∞, and the corrected activities referred to the center of the uranium slug, A_o. The radial distances along the P, Q and R radials were designated p, q and r respectively. Various combinations of experimental data are plotted in Figures 6 through 29. In fairing curves through the experimental points it was assumed that there were no radical changes of curvature of the flux distribution within the graphite block.

A. Effect of Foil Spacing

Figure 6 indicates that induced activities for foil spacings 1 and 2 along the P radial were approximately the same and that they were about 5 per cent lower than the induced activities of those foils irradiated at spacing 3. This depression increased to approximately 10 per cent for those foils located closest to the fuel assembly. Along the Q radial the change in foil spacing had an effect on the induced activities as is shown in Figure 7. Along the R radial there was approximately a 5 per cent decrease in induced activities of foils irradiated at spacing 1 compared to those

Figure 6. Effect of foil spacing along P radial

Runs made without coolant, using medium foils oriented horizontally

Run no.	Spacing
1	1
2	2
3	3

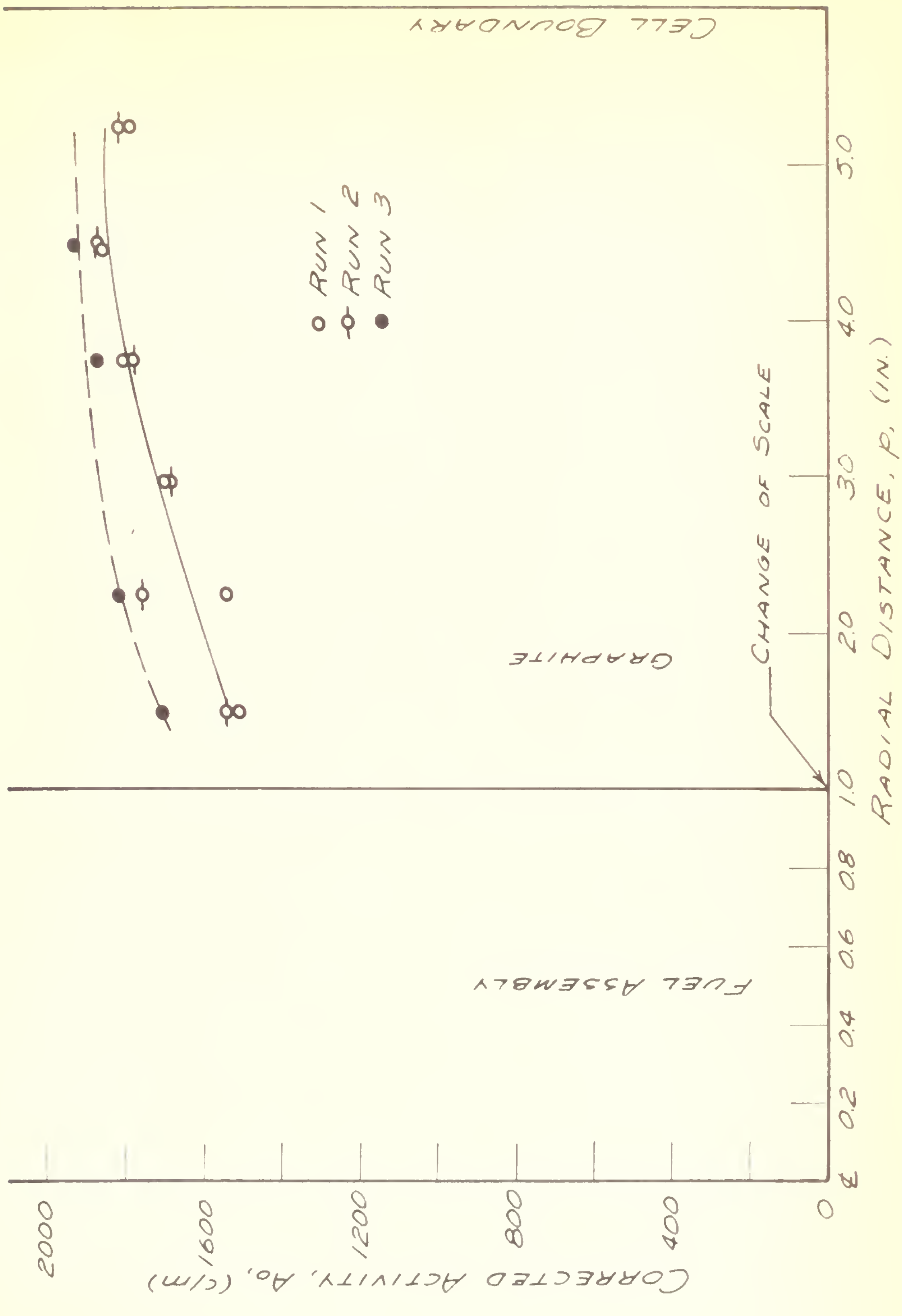
CELL BOUNDARY
GRAPHITE
FUEL ASSEMBLY
CHANGE OF SCALE
○ RUN 1
-○- RUN 2
● RUN 3
RADIAL DISTANCE, ρ, (IN.)
℄
0.2
0.4
0.6
0.8
1.0
2.0
3.0
4.0
5.0
CORRECTED ACTIVITY, A₀, (c/m)
0
400
800
1200
1600
2000

Figure 7. Effect of foil spacing along Q radial

Runs made without coolant, using medium foils oriented horizontally

Run no.	Spacing
6	1
7	3

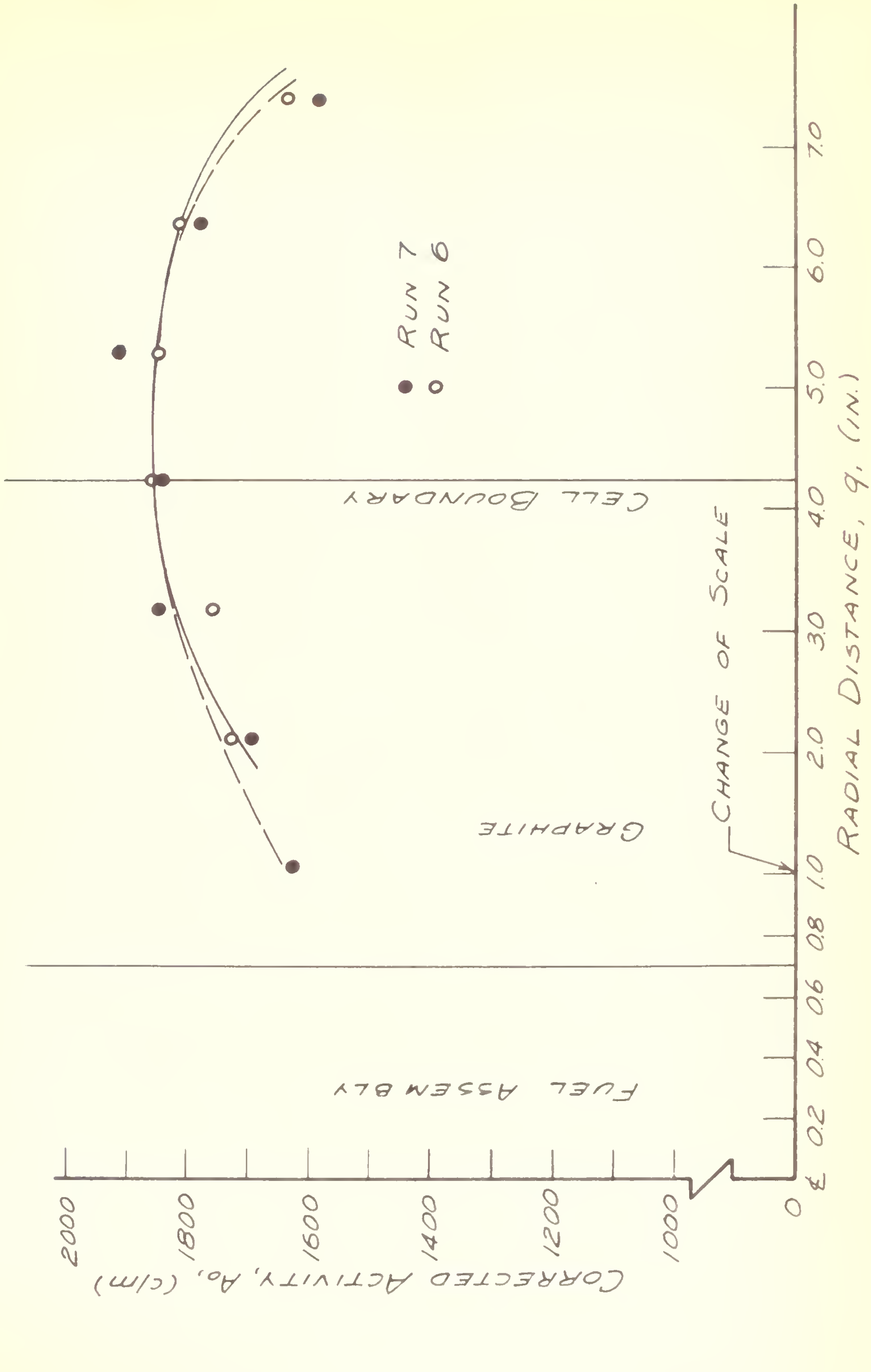
Corrected Activity, A_0, (c/m)
2000
1800
1600
1400
1200
1000
0
Radial Distance, q, (in.)
℄
0.2
0.4
0.6
0.8
1.0
2.0
3.0
4.0
5.0
6.0
7.0
Fuel Assembly
Graphite
Cell Boundary
Change of Scale
● Run 7
○ Run 6

irradiated at spacing 2 as indicated in Figure 8.

On run 4 medium foils were close packed on the [illegible] radial in the fuel assembly and were placed at spacing 1 in the graphite. Figure 9 compares the activities obtained on this run with those obtained on runs 1 and 5 where the foil spacing 1 was used in the graphite and normal spacing was used in the fuel assembly. There was apparently a 10 to 15 per cent depression of foil activity in the fuel assembly and a 10 to 20 per cent increase in foil activity in the graphite. The same type of runs was made and compared on the A radial in Figure 10. There was a 15 to 20 per cent depression of activities in the fuel assembly with the foils close packed, but in the graphite the activities were about the same. The above runs were all dry runs. Figures 11, 12 and 13 show the results of similar runs that were made with water in the coolant annulus. Approximately a 10 per cent depression in the induced activities was again noted when the foils were close packed in the fuel assembly, but there was very little change in the activities of those foils placed in the graphite. There did not appear to be a great deal of distortion of the flux pattern by placing the foils close packed in the fuel assembly.

Figure 8. Effect of foil spacing along R radial

Runs made without coolant, using medium foils oriented vertically

Run no.	Spacing
12	1
13	2

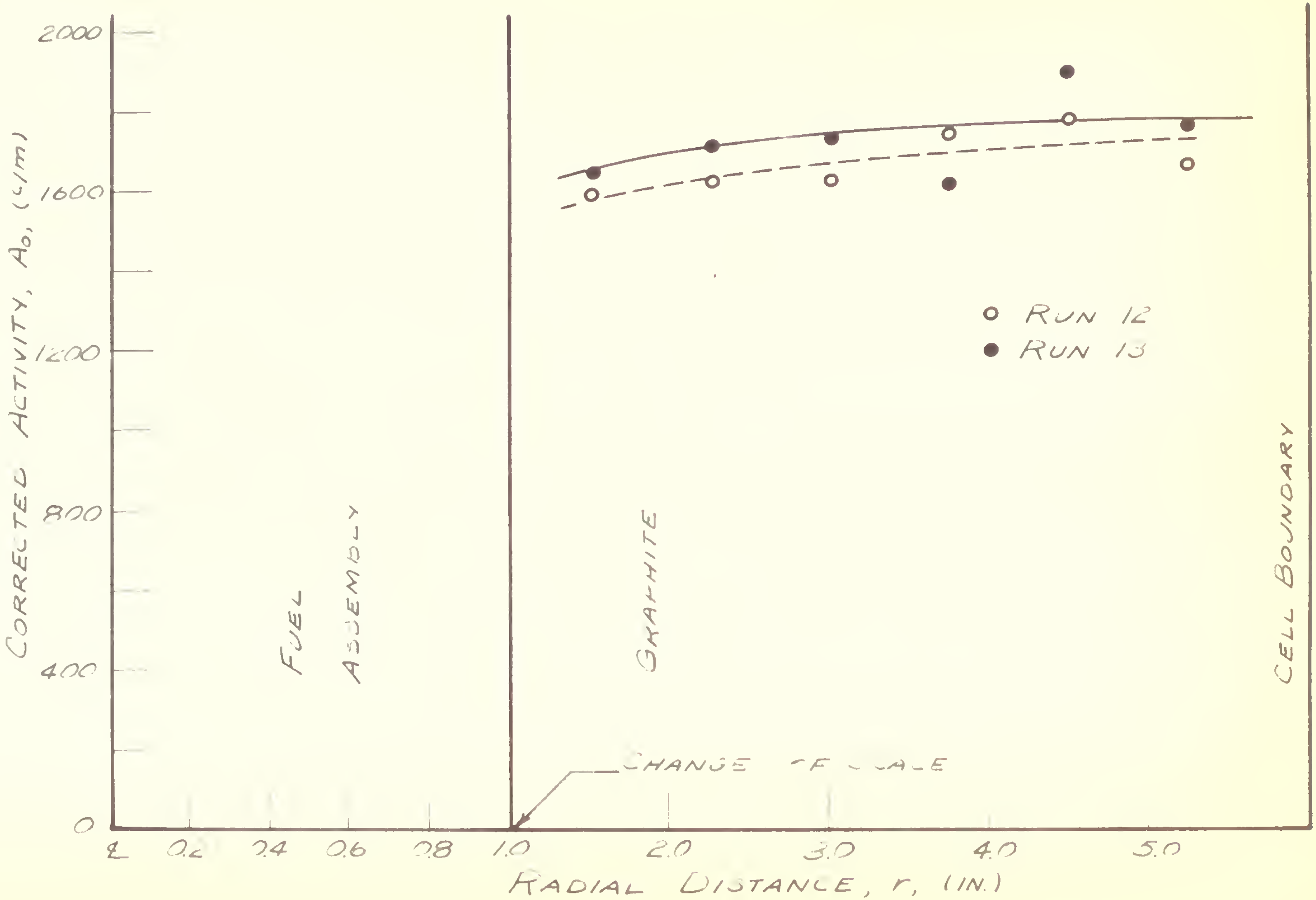
2000
1600
1200
800
400
0
CORRECTED ACTIVITY, A_0, (c/m)
℄
0.2
0.4
0.6
0.8
1.0
2.0
3.0
4.0
5.0
RADIAL DISTANCE, r, (IN.)
FUEL ASSEMBLY
GRAPHITE
CELL BOUNDARY
CHANGE OF SCALE
○ RUN 12
● RUN 13

Figure 9. Effect of foil spacing along P radial

Runs made without coolant, using medium foils

Run no.	Region	Spacing	Orientation
4	graphite	1	vertical
4	fuel assembly	close packed	radial
1	graphite	1	vertical
5	fuel assembly	normal	radial

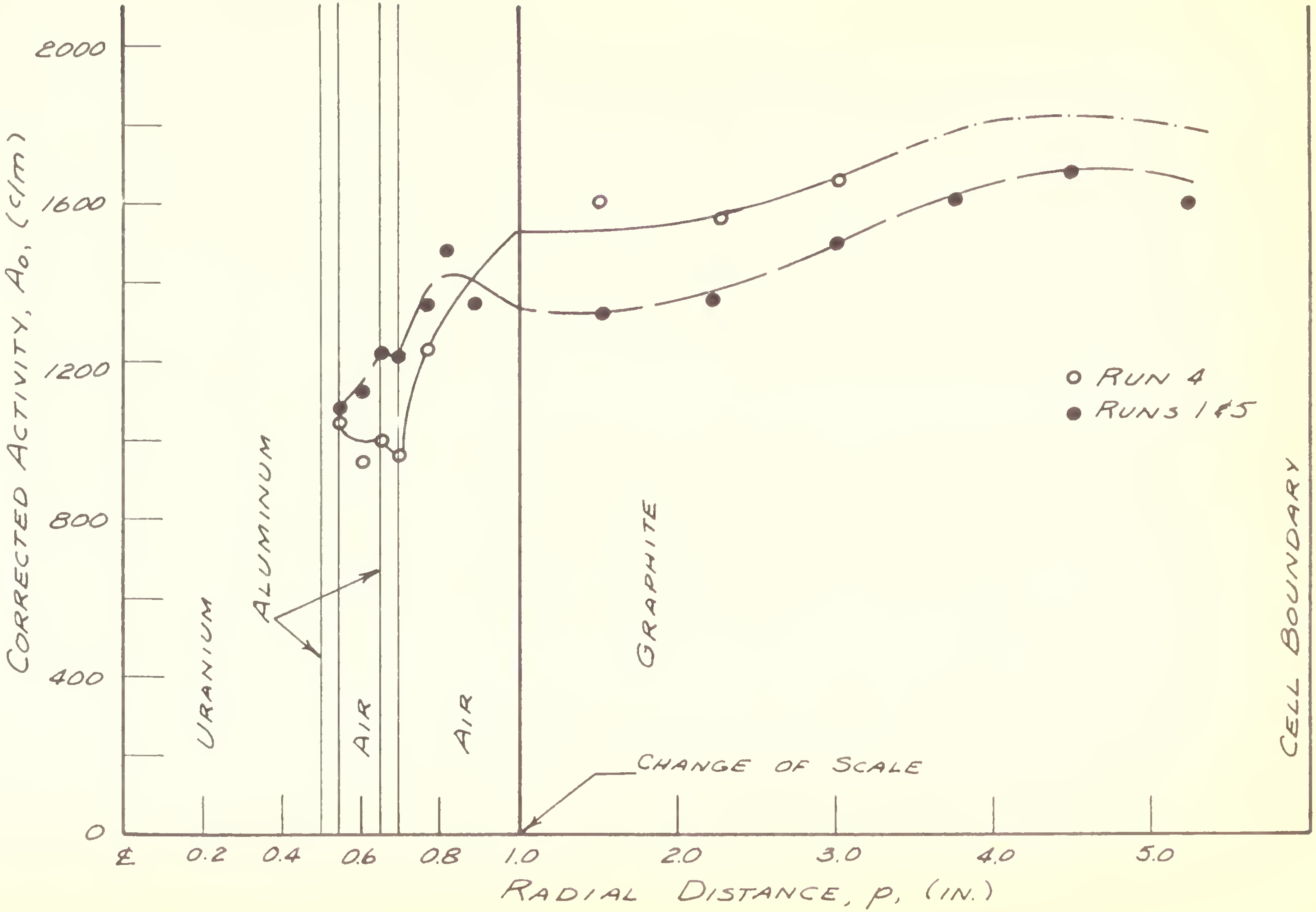
CORRECTED ACTIVITY, A_0, (c/m)
2000
1600
1200
800
400
0
℄
0.2
0.4
0.6
0.8
1.0
2.0
3.0
4.0
5.0
RADIAL DISTANCE, ρ, (IN.)
URANIUM
ALUMINUM
AIR
AIR
GRAPHITE
CHANGE OF SCALE
CELL BOUNDARY
○ RUN 4
● RUNS 1 & 5

Figure 10. Effect of foil spacing along R radial

Runs made without coolant, using medium foils

Run no.	Region	Spacing	Orientation
15	graphite	1	vertical
15	fuel assembly	close packed	radial
12	graphite	1	vertical
16	fuel assembly	normal	radial

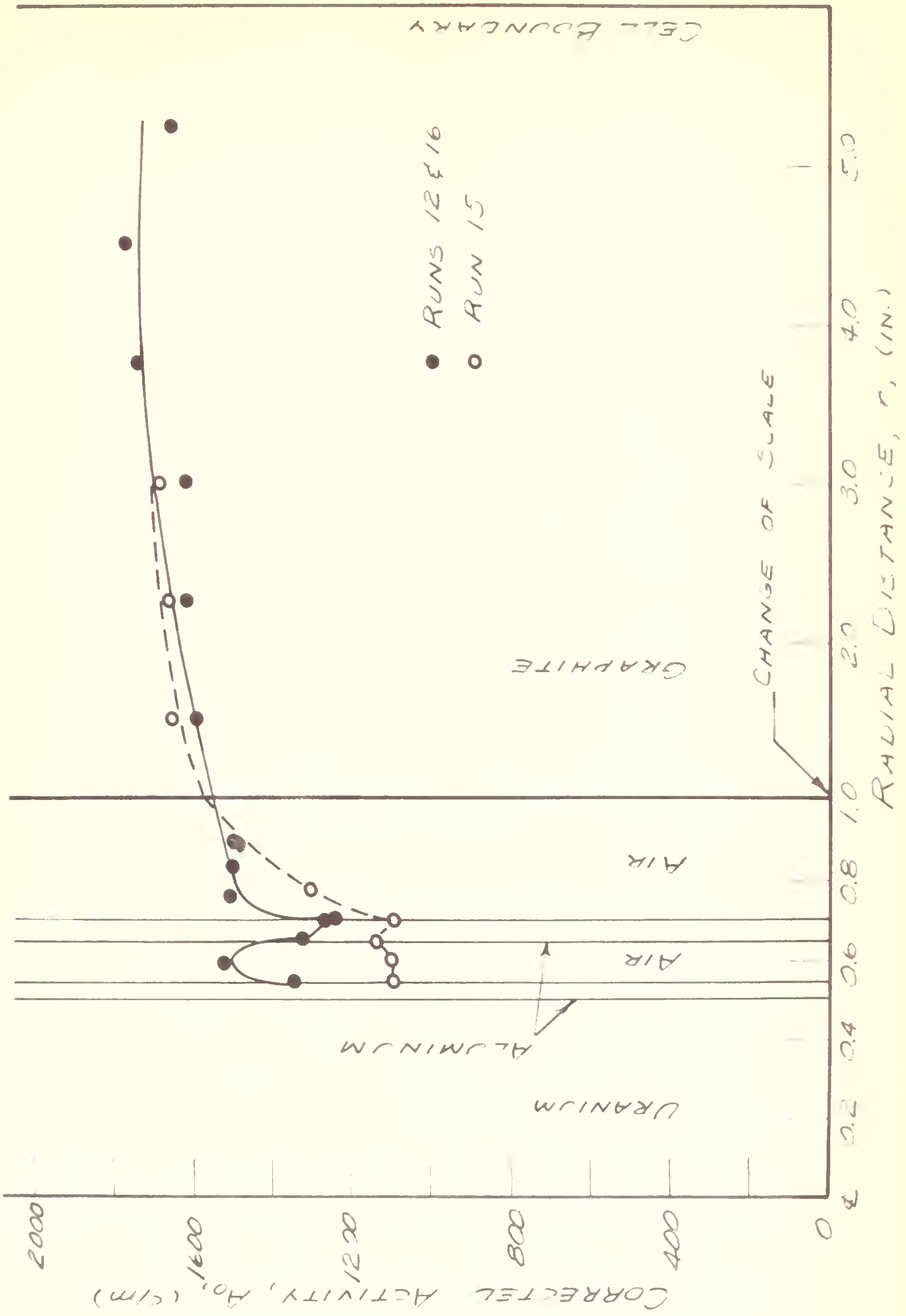
CELL BOUNDARY
● RUNS 12 & 16
○ RUN 15
GRAPHITE
AIR
AIR
ALUMINUM
URANIUM
CHANGE OF SCALE
RADIAL DISTANCE, r, (IN.)
℄
0.2
0.4
0.6
0.8
1.0
2.0
3.0
4.0
5.0
CORRECTED ACTIVITY, A_0, (c/m)
0
400
800
1200
1600
2000

Figure 11. Effect of foil spacing along P radial

Runs made with water coolant, using medium foils (large foils were used in positions P1, P2 and P3 on run 20)

Run no.	Region	Spacing	Foil orientation
19	graphite	1	horizontal
19	fuel assembly	close packed	radial
18	graphite	2	horizontal
20	fuel assembly	normal	radial

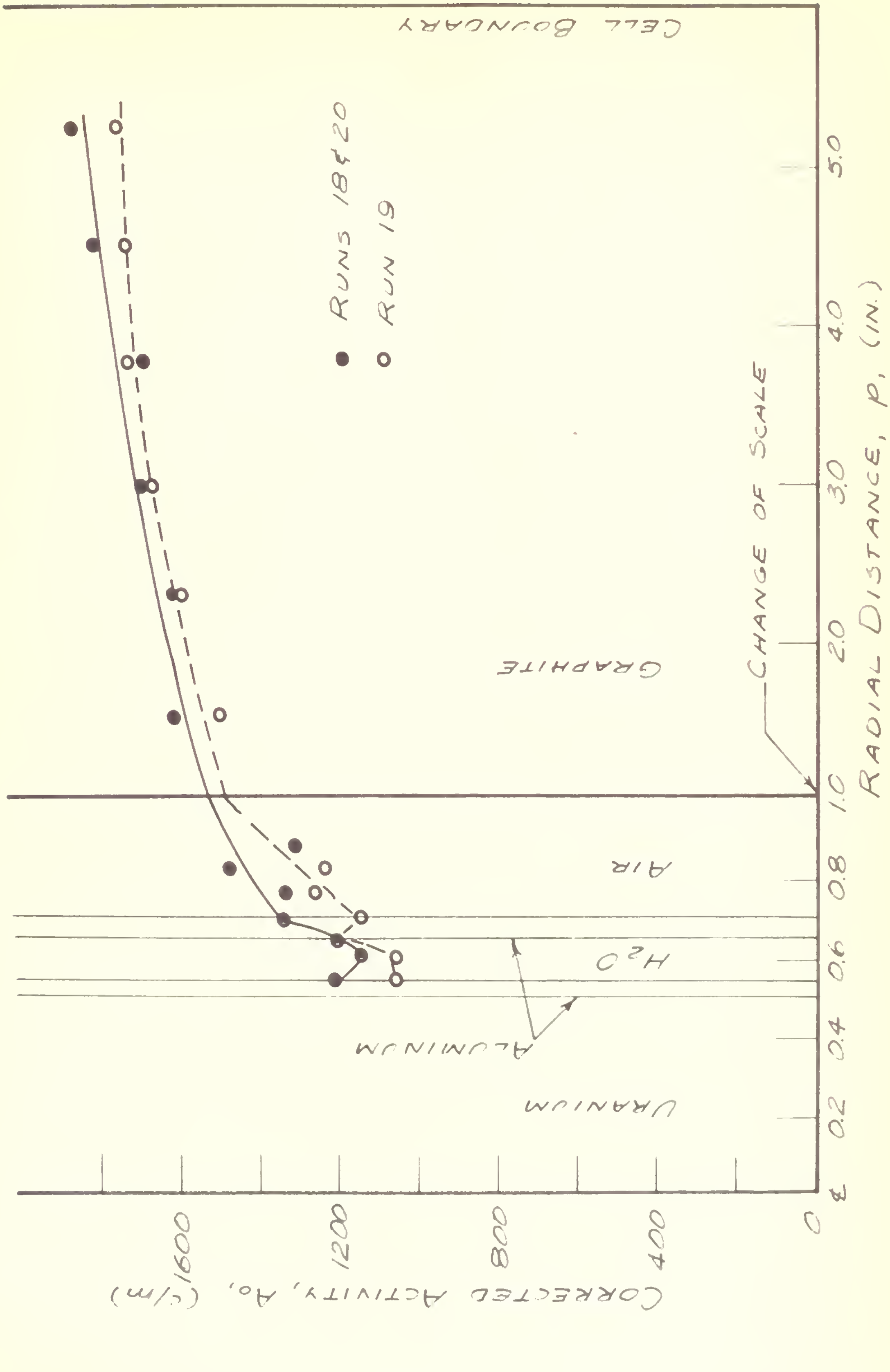
CELL BOUNDARY
● RUNS 18 & 20
○ RUN 19
GRAPHITE
AIR
H_2O
ALUMINUM
URANIUM
CHANGE OF SCALE
RADIAL DISTANCE, ρ, (IN.)
℄
0.2
0.4
0.6
0.8
1.0
2.0
3.0
4.0
5.0
CORRECTED ACTIVITY, A_0, (c/m)
0
400
800
1200
1600

Figure 12. Effect of foil spacing along Q radial

Runs were made with water coolant, using medium foils (large foils were used in positions Q1 and Q2 on run 26)

Run no.	Region	Spacing	Fuel orientation
25	graphite	1	horizontal
25	fuel assembly	close packed	radial
23	graphite	3	horizontal
26	fuel assembly	normal	radial

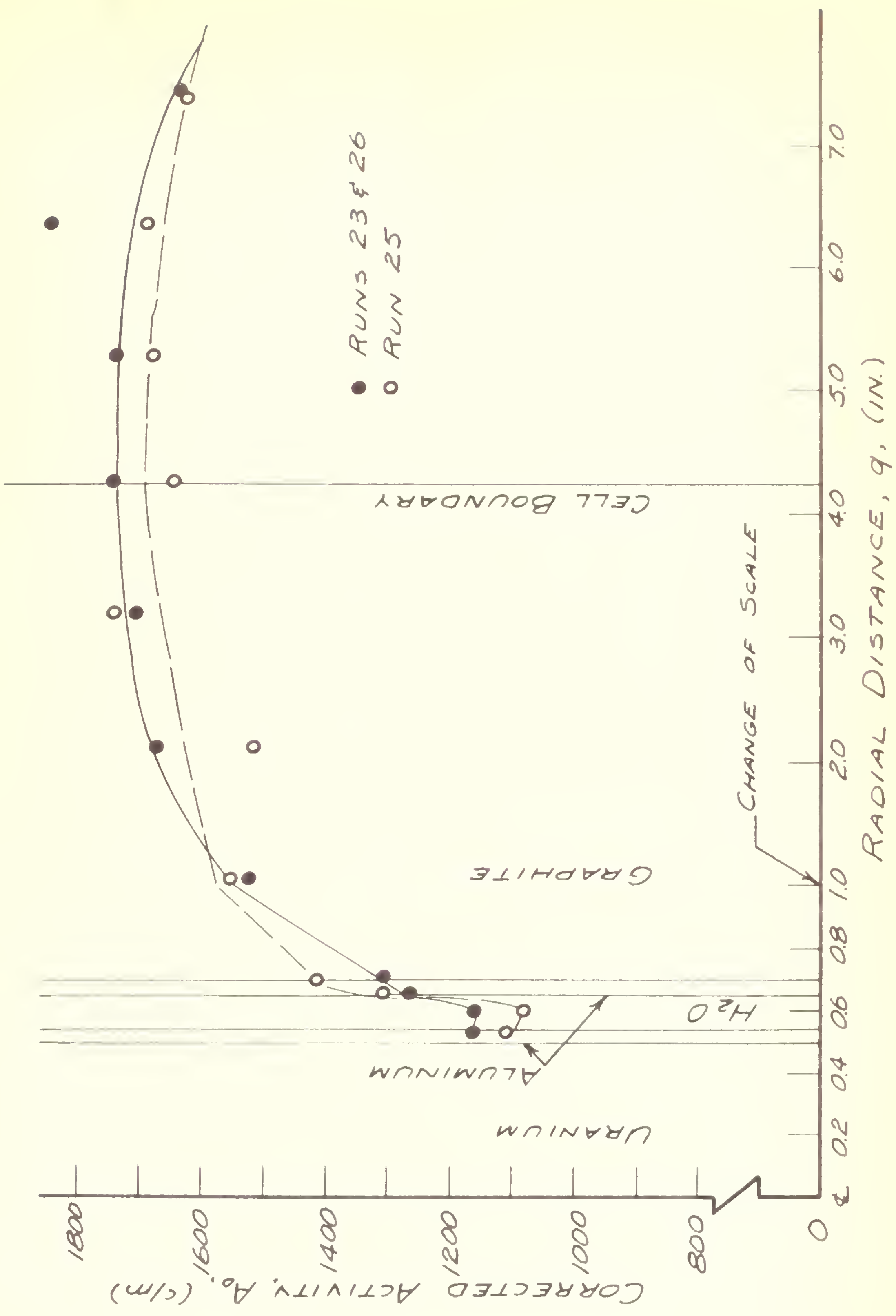
CORRECTED ACTIVITY, A_o, (c/m)
1800
1600
1400
1200
1000
800
0
RADIAL DISTANCE, q, (IN.)
℄
0.2
0.4
0.6
0.8
1.0
2.0
3.0
4.0
5.0
6.0
7.0
URANIUM
ALUMINUM
H_2O
GRAPHITE
CELL BOUNDARY
CHANGE OF SCALE
● RUNS 23 & 26
○ RUN 25

Figure 13. Effect of foil spacing along R radial

Runs were made with water coolant, using medium foils (large foils were used in positions R4, R5 and R6 on run 31)

Run no.	Region	Spacing	Orientation
30	graphite	1	vertical
30	fuel assembly	close packed	radial
29	graphite	2	vertical
31	fuel assembly	normal	radial

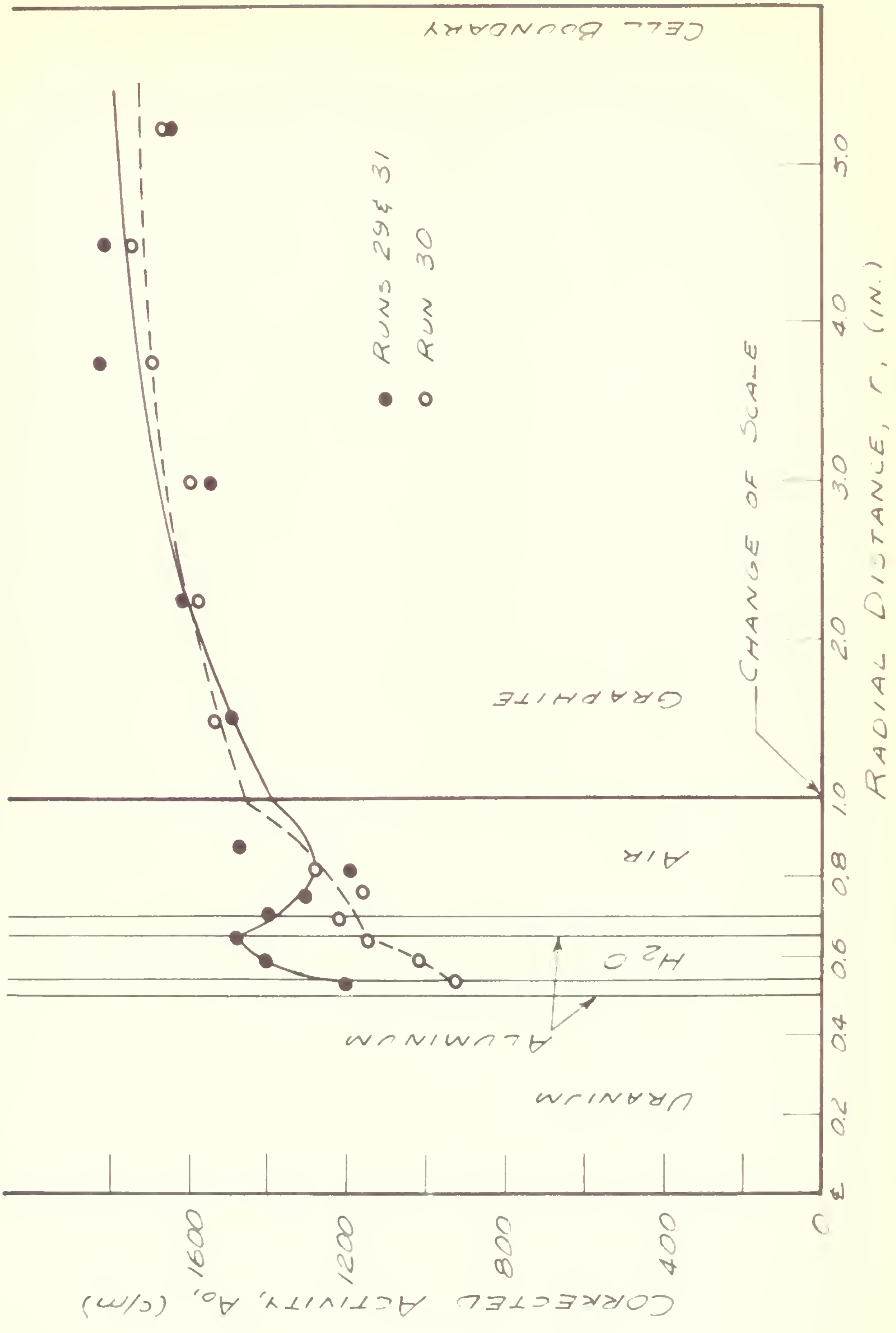
CELL BOUNDARY
● RUNS 29 & 31
○ RUN 30
GRAPHITE
AIR
H_2O
ALUMINUM
URANIUM
CHANGE OF SCALE
RADIAL DISTANCE, r, (IN.)
℄
0.2
0.4
0.6
0.8
1.0
2.0
3.0
4.0
5.0
CORRECTED ACTIVITY, A_0, (c/m)
0
400
800
1200
1600

B. Effect of Foil Orientation

Runs 6, 8 and 10 were dry runs made along the Q radial with medium foils placed in the graphite in a horizontal position, vertical position and an L-shaped position respectively. The horizontal and vertical placement gave very nearly the same distribution along the radial as shown in Figure 14. The L-shaped foil orientation appeared to result in activities that were depressed approximately 10 per cent from those obtained from the horizontal and vertical positions. The activities from the L-shaped foils also had a larger amount of scatter than those activities obtained from foils mounted horizontally or vertically.

C. Effect of Foil Size

Large, medium and small foils were used on runs 22, 23 and 24 in the graphite on the Q radial with spacing 3. Figure 15 shows that the small foils resulted in the highest specific activity, with the medium foil specific activities being depressed approximately 10 per cent from these and the large foil activities being depressed 15 to 20 per cent from the small foil activities. This trend was not observed on the P radial where on runs 17 and 18 using large and medium foils respectively, with spacing 2, almost identical flux

Figure 14. Effect of foil orientation

Runs made along Q radial, without coolant, using medium foils at spacing 1

Run no.	Orientation
6	horizontal
8	vertical
10	L-shaped

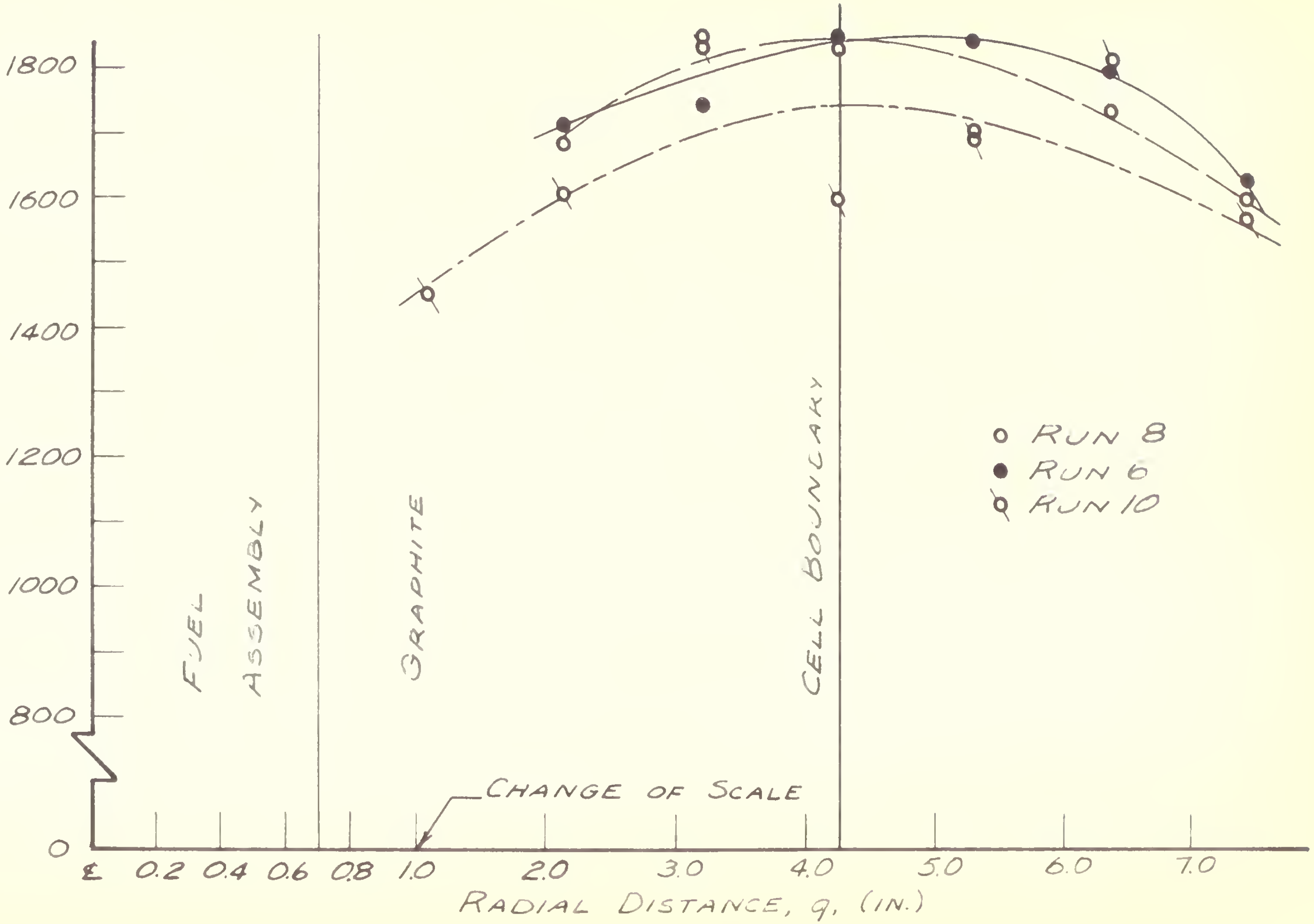
1800
1600
1400
1200
1000
800
0
℄
0.2
0.4
0.6
0.8
1.0
2.0
3.0
4.0
5.0
6.0
7.0
RADIAL DISTANCE, q, (IN.)
FUEL ASSEMBLY
GRAPHITE
CELL BOUNDARY
CHANGE OF SCALE
○ RUN 8
● RUN 6
ϙ RUN 10

Figure 15. Effect of foil size along Q radial

Runs made with water coolant at foil spacing 3 with foils oriented horizontally

Run no.	Foil size
22	large
23	medium
24	small

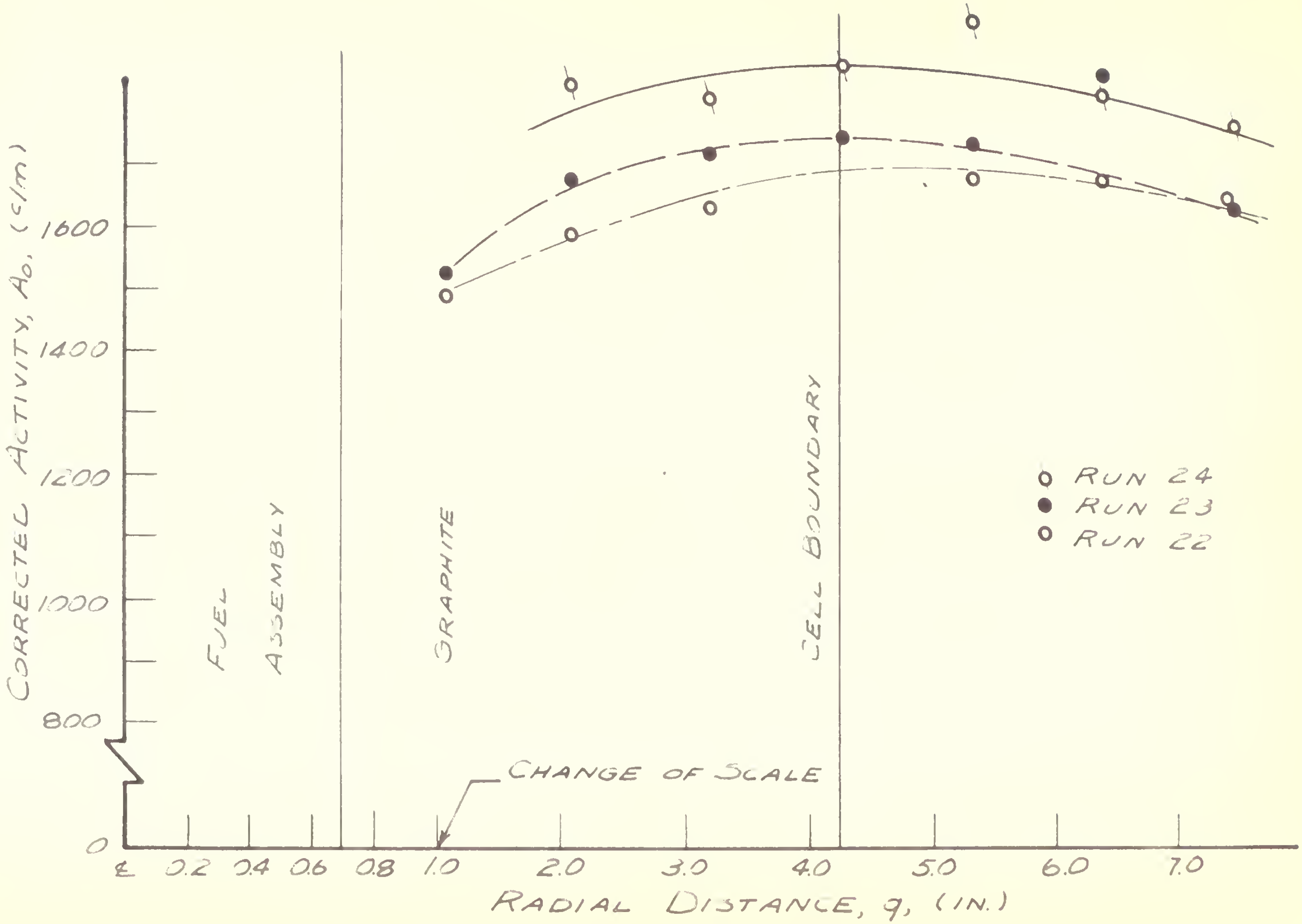
Corrected Activity, A_0, (c/m)
1600
1400
1200
1000
800
0
Fuel Assembly
Graphite
Cell Boundary
Run 24
Run 23
Run 22
Change of Scale
℄
0.2
0.4
0.6
0.8
1.0
2.0
3.0
4.0
5.0
6.0
7.0
Radial Distance, q, (in.)

distribution curves were obtained along the radial as shown in Figure 16. Figure 17 is a plot of runs 28 and 29 which were the same as runs 17 and 18 except that they were taken along the H radial. In this instance the large foil activities were found to be 12 per cent less than the medium foil activities. For run 21 small foils were placed in the fuel assembly one at a time along the P radial. The activities obtained in this manner were not appreciably different from those obtained with medium foils placed two at a time in the fuel element assembly, as can be seen by comparing run 21 with run 20 in Figure 16.

D. Variation of Flux Along Different Radials

In an isolated unit cell with cylindrical geometry the lines of constant flux in the moderator would be concentric circles. In a square unit cell in a reactor the lines of constant flux in the moderator in the vicinity of the fuel assembly are closely approximated by concentric circles if the overall flux in the reactor were uniform from cell to cell. (3, p. 79) As the unit cell boundary is approached the lines of constant flux are gradually distorted from circles into squares. At the cell boundarythe lines of constant flux would be squares. Since the unit cell activities, A_o, have all been corrected for the cosine

Figure 16. Effect of foil size along P radial

Runs made with water coolant, foils oriented horizontally with normal foil spacing in the fuel assembly and spacing 2 in the graphite

Run no.	Foil size
17	large
18	medium
20	medium
21	small

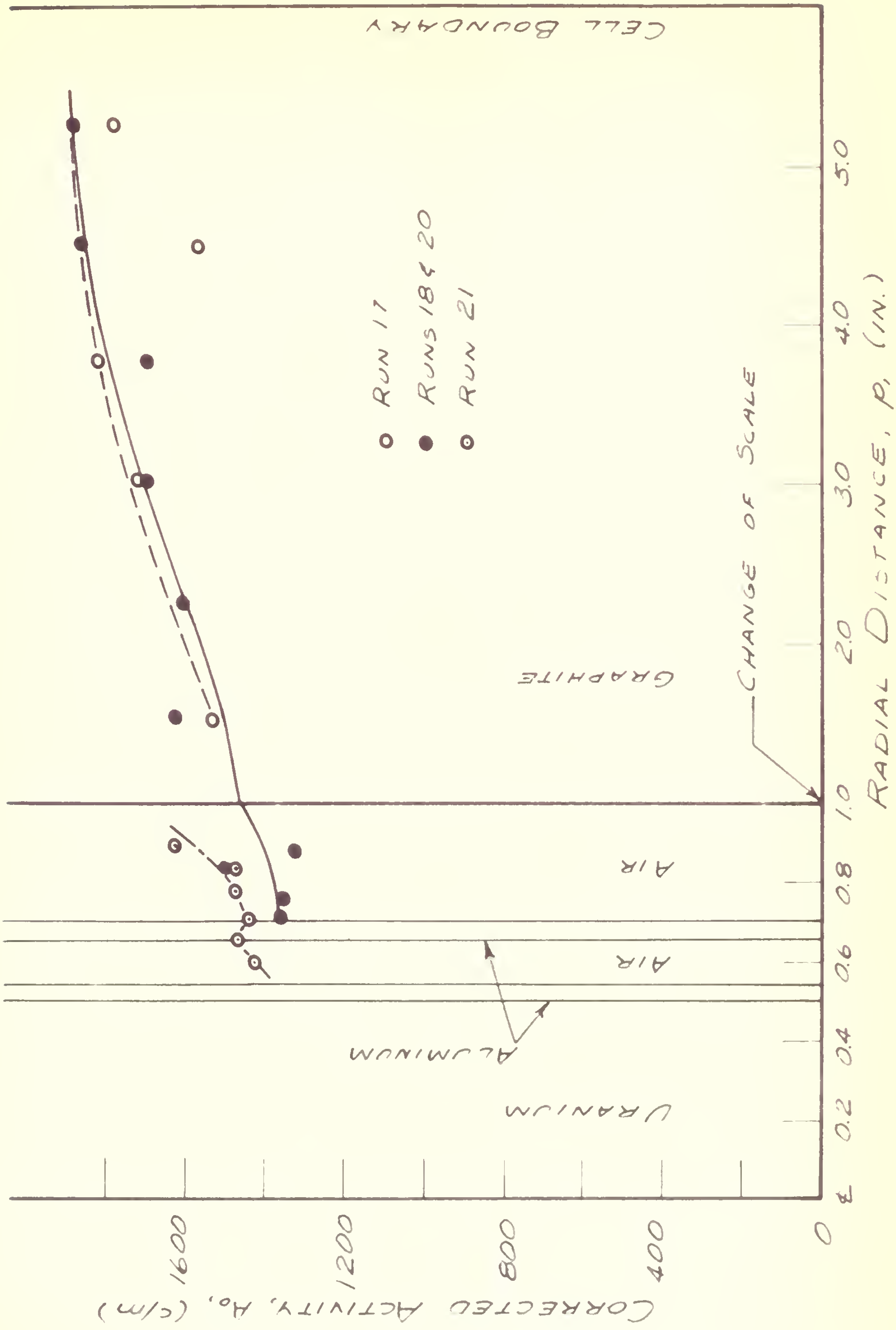
CELL BOUNDARY
GRAPHITE
AIR
AIR
ALUMINUM
URANIUM
CHANGE OF SCALE
○ RUN 17
● RUNS 18 & 20
⊙ RUN 21
℄
0.2
0.4
0.6
0.8
1.0
2.0
3.0
4.0
5.0
RADIAL DISTANCE, ρ, (IN.)
0
400
800
1200
1600
CORRECTED ACTIVITY, A_0, (c/m)

Figure 17. Effect of foil size along R radial

Runs were made with water coolant, foils oriented vertically at specing 2

Run no.	Foil size
28	large
29	medium

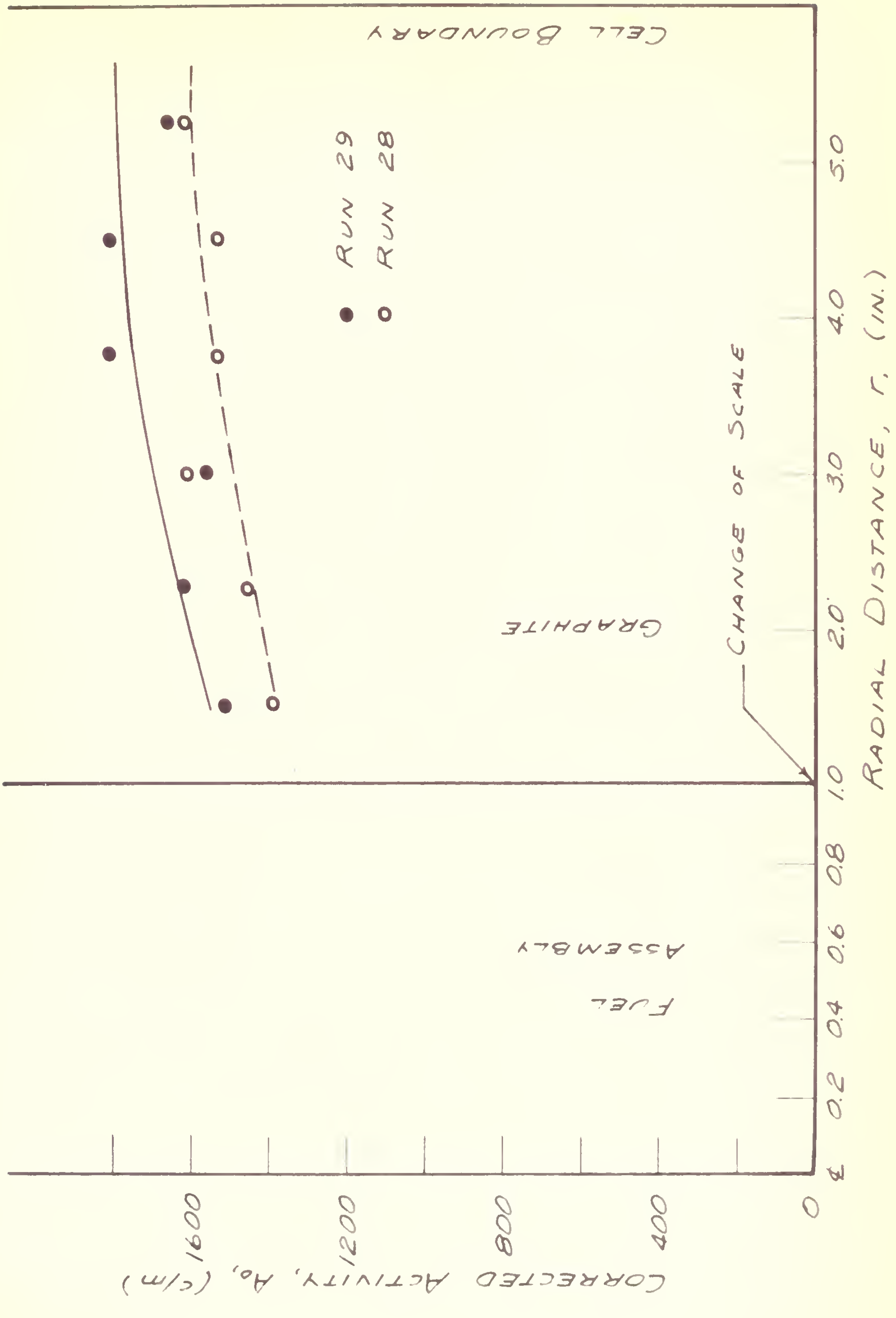
CORRECTED ACTIVITY, A₀, (c/m)
0
400
800
1200
1600
RADIAL DISTANCE, r, (IN.)
℄
0.2
0.4
0.6
0.8
1.0
2.0
3.0
4.0
5.0
CELL BOUNDARY
GRAPHITE
FUEL ASSEMBLY
CHANGE OF SCALE
● RUN 29
○ RUN 28

distribution in the x direction and the exponential drop in the z direction, these activities correspond to those which would be obtained if the flux in the overall assembly were uniform. Therefore lines of constant flux (or corrected activity) should be very nearly concentric circles near the fuel assembly. Since the lines of constant flux are compressed along the Q radial as they change from circular to square shape, it should be expected that at a given radial distance the flux along the P and R radials would be equal but less than the flux along the Q radial.

In Figures 18 and 19 the corrected foil activities along the P, Q and R radials are plotted and compared for the wet and dry runs respectively. The activities along the different radials are seen to match up very closely for the wet runs and fairly well for the dry runs. Activities along the Q radial appeared to be slightly higher than on the P and R radials. This was probably due to the reason mentioned above and to the fact that spacing 3 was used on the Q radial while spacing 2 was used on the P and R radials. The activities of the foils in the fuel assembly all fell within relatively narrow limits as can be seen in Figures 18 and 19. The single curve faired through these points in the fuel assembly corresponds to the average at a given radial distance of the activities measured along the three radials. Figures 20 and 21 are the same as 18 and 19 except that on these runs the

Figure 18. Variation of flux with radial direction without coolant

Runs made using medium foils

Run no.	Radial	Region	Spacing	Orientation
2	P	graphite	2	horizontal
5	P	fuel assembly	normal	radial
7	Q	graphite	3	horizontal
11	Q	fuel assembly	normal	radial
13	R	graphite	2	vertical
16	R	fuel assembly	normal	radial

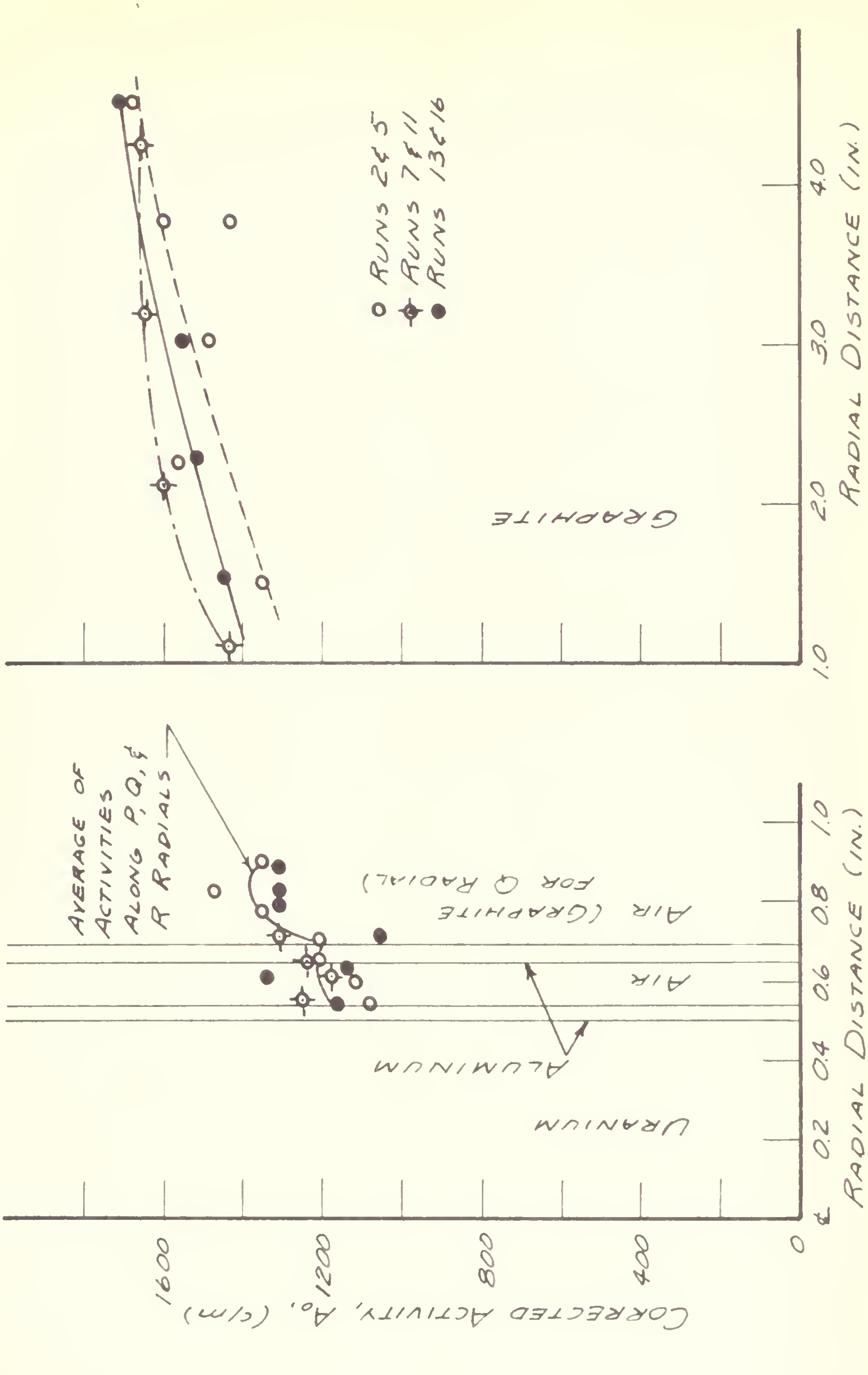
CORRECTED ACTIVITY, A₀, (c/m)
0
400
800
1200
1600
RADIAL DISTANCE (IN.)
℄
0.2
0.4
0.6
0.8
1.0
RADIAL DISTANCE (IN.)
1.0
2.0
3.0
4.0
URANIUM
ALUMINUM
AIR
AIR (GRAPHITE FOR Q RADIAL)
GRAPHITE
AVERAGE OF ACTIVITIES ALONG P, Q, & R RADIALS
○ RUNS 2 & 5
⊕ RUNS 7 & 11
● RUNS 13 & 16

Figure 19. Variation of flux with radial direction with water coolant

Runs made using medium foils

Run no.	Radial	Region	Spacing	Orientation
18	P	graphite	2	horizontal
20	P	fuel assembly	normal	radial
23	Q	graphite	3	horizontal
26	Q	fuel assembly	normal	radial
29	R	graphite	2	vertical
31	R	fuel assembly	normal	radial

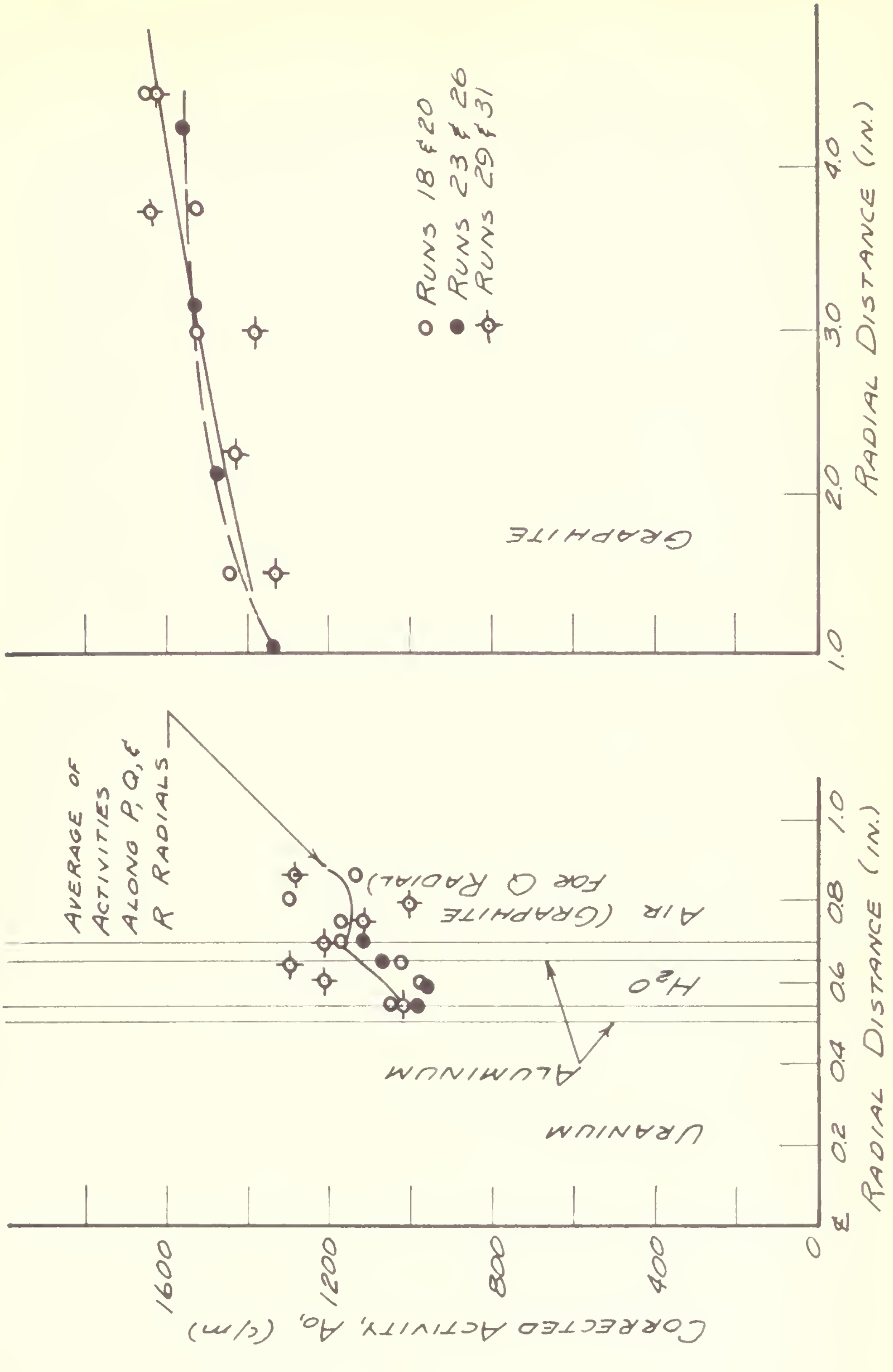
CORRECTED ACTIVITY, A_o, (c/m)
1600
1200
800
400
0
℄
0.2
0.4
0.6
0.8
1.0
RADIAL DISTANCE (IN.)
1.0
2.0
3.0
4.0
RADIAL DISTANCE (IN.)
URANIUM
ALUMINUM
H_2O
AIR (GRAPHITE FOR Q RADIAL)
AVERAGE OF ACTIVITIES ALONG P, Q, & R RADIALS
GRAPHITE
○ RUNS 18 & 20
● RUNS 23 & 26
⊕ RUNS 29 & 31

Figure 20. Variation of flux with radial direction without coolant

Runs made using medium foils at spacing 1 in the graphite and close packed in the fuel assembly

Run no.	Radial	Foil orientation
4	P	horizontal
15	R	vertical

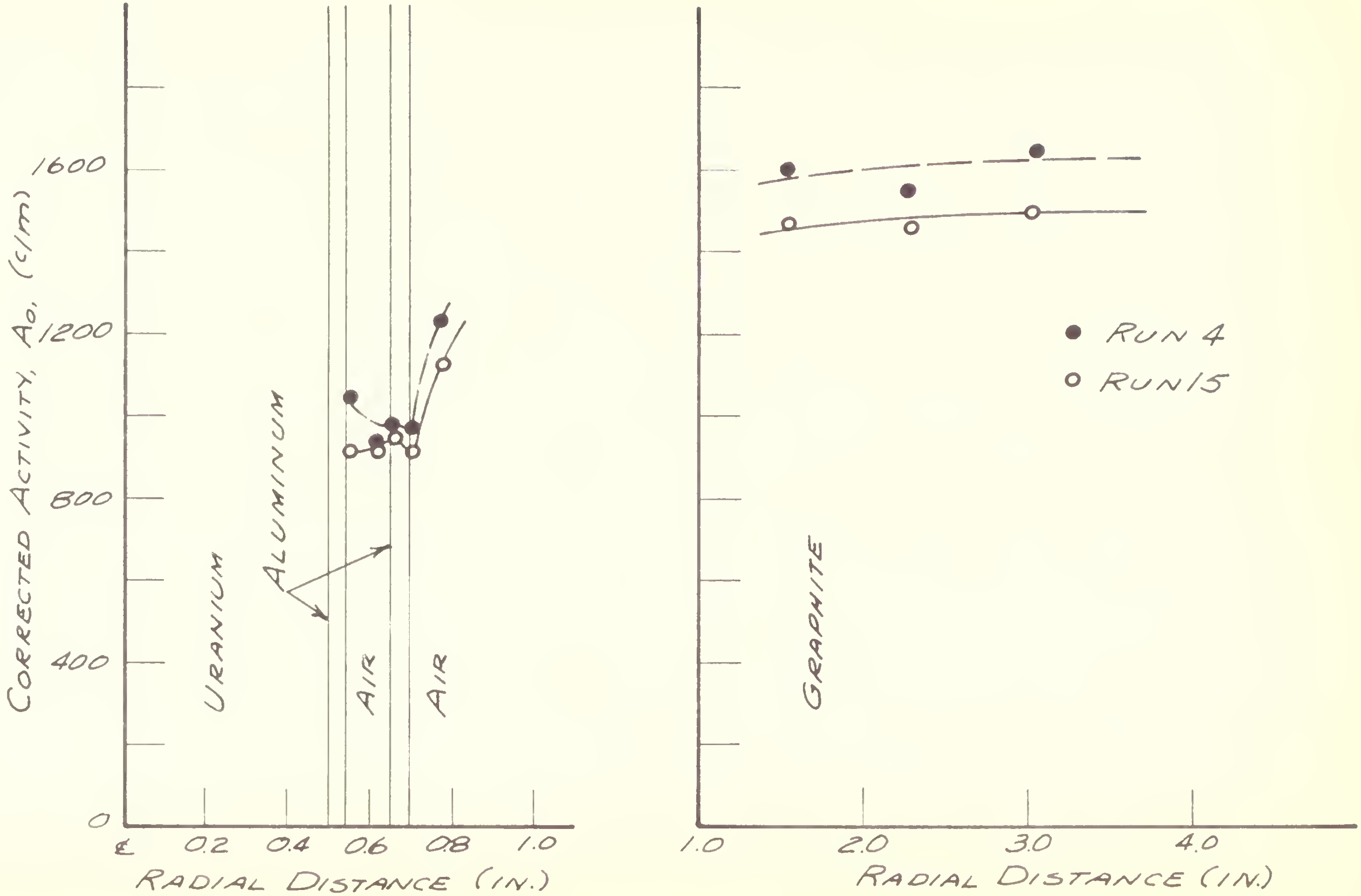
Corrected Activity, A_o, (c/m)
1600
1200
800
400
0
Uranium
Aluminum
Air
Air
℄
0.2
0.4
0.6
0.8
1.0
Radial Distance (in.)
Graphite
● Run 4
○ Run 15
1.0
2.0
3.0
4.0
Radial Distance (in.)

Figure 21. Variation of flux with radial direction with water coolant with foils close packed in the fuel assembly and at spacing 1 in the graphite

Run no.	Radial	Foil orientation
19	P	horizontal
25	Q	horizontal
30	R	vertical

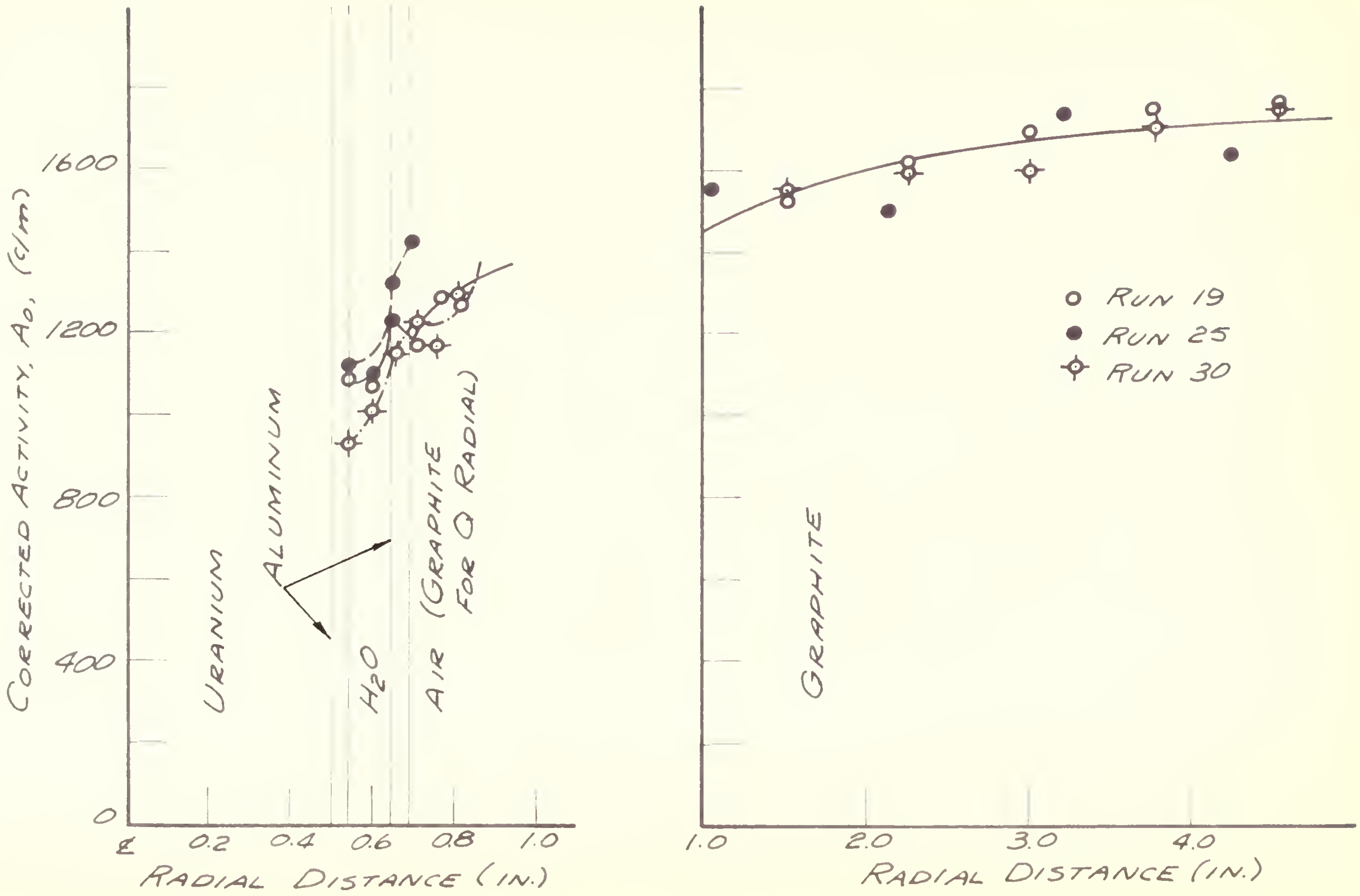
Corrected Activity, A₀, (c/m)
1600
1200
800
400
0
℄
0.2
0.4
0.6
0.8
1.0
Radial Distance (in.)
Uranium
Aluminum
H₂O
Air (Graphite
for ℄ Radial)
Graphite
1.0
2.0
3.0
4.0
Radial Distance (in.)
○ Run 19
● Run 25
⌖ Run 30

foils in the fuel assembly were close packed. These runs simply corroborated the results shown in Figures 18 and 19. The average activities in the fuel assembly are seen to agree very closely in general shape, but the magnitudes of the close packed foil activities are depressed 10 to 15 per cent below the activities of those foils that were irradiated only two at a time. See also Figure 27 which compares the averages of the above runs.

E. Effect of Coolant

Identical runs were made along each radial with and without coolant and these are plotted in Figures 22, 23 and 24. On the wet runs there appeared to be about a 5 per cent depression in the flux in the region adjacent to the fuel assembly along all three radials. This depression continued to the unit cell boundary on the Q radial, but there was no apparent depression at the unit cell boundary on the P and R radials.

Within the fuel assembly it could in general be said that the flux was depressed on the wet runs. On the P and Q radials this depression amounted to about 10 per cent whereas on the R radial the depression was very slight. There was a characteristic flux pattern evident in the fuel assembly from the data for the individual runs which was more apparent

Figure 22. Effect of coolant along P radial

Runs were made using medium foils (large foils were used in positions P1, P2 and P3 on run 20) at normal spacing in fuel assembly and spacing 2 in the graphite

Run no.	Coolant	Region	Foil orientation
2	None	graphite	horizontal
5	None	fuel assembly	radial
18	Water	graphite	horizontal
20	Water	fuel assembly	radial

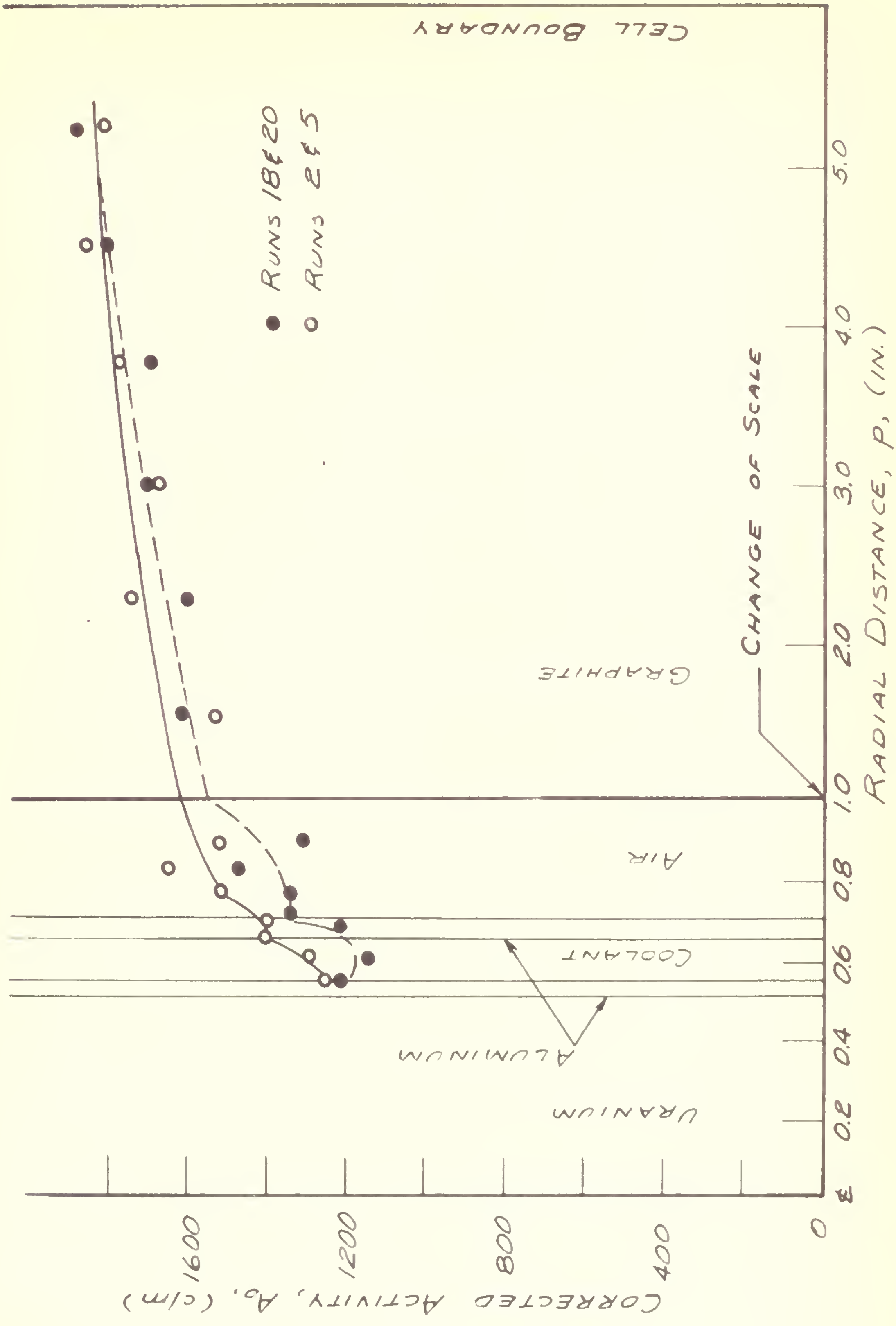
CELL BOUNDARY
● RUNS 18 & 20
○ RUNS 2 & 5
CHANGE OF SCALE
GRAPHITE
AIR
COOLANT
ALUMINUM
URANIUM
℄
0.2
0.4
0.6
0.8
1.0
2.0
3.0
4.0
5.0
RADIAL DISTANCE, ρ, (IN.)
0
400
800
1200
1600
CORRECTED ACTIVITY, A_0, (c/m)

Figure 23. Effect of coolant along Q radial

Runs were made using medium foils (large foils were used in positions Q1 and Q2 on run 26)

Run no.	Coolant	Region	Foil orientation	Spacing
7	None	graphite	horizontal	normal
11	None	fuel assembly	radial	3
23	Water	graphite	horizontal	normal
26	Water	fuel assembly	radial	3

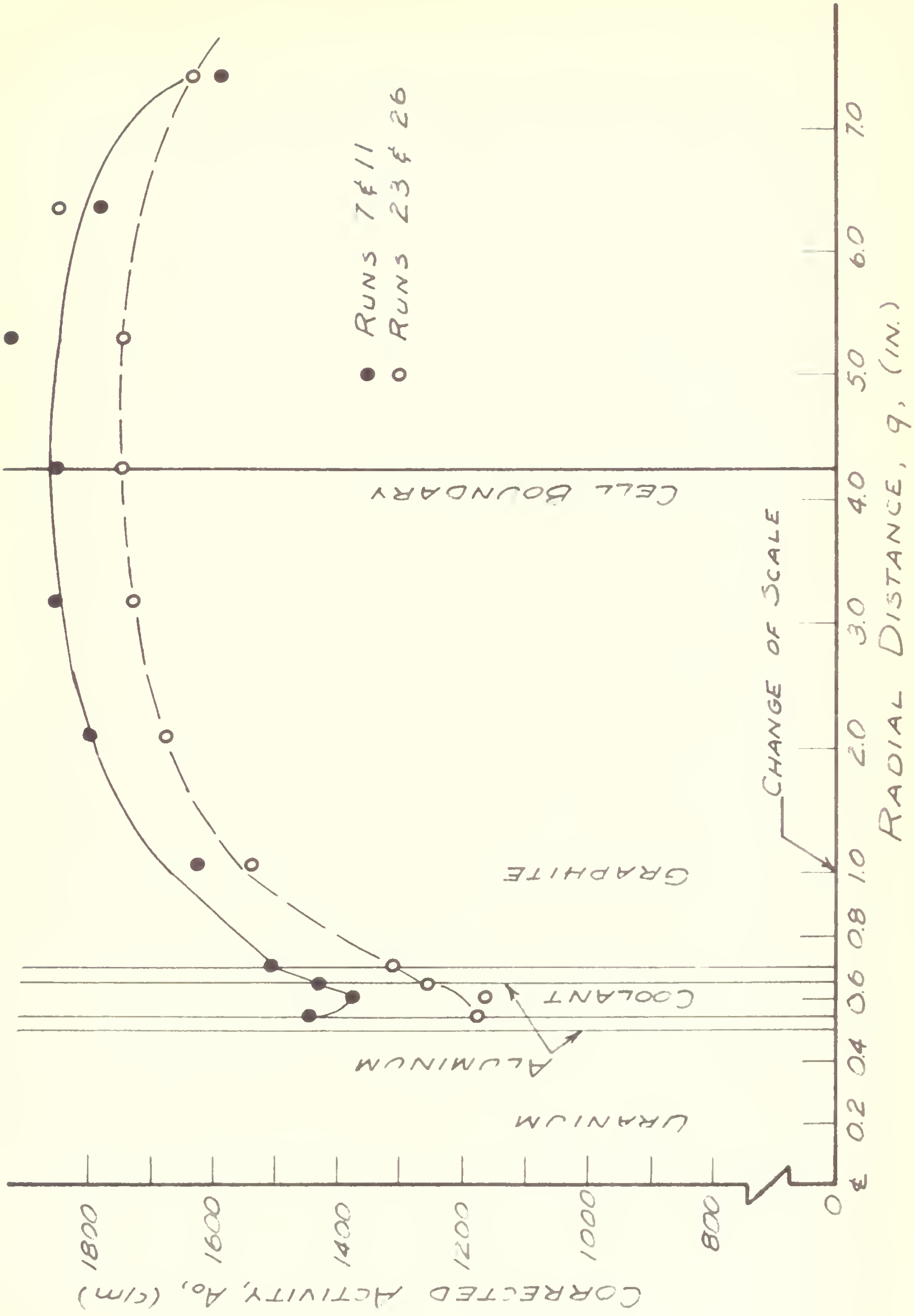
CORRECTED ACTIVITY, Ao, (C/M)
1800
1600
1400
1200
1000
800
0
RADIAL DISTANCE, 9, (IN.)
℄
0.2
0.4
0.6
0.8
1.0
2.0
3.0
4.0
5.0
6.0
7.0
● RUNS 7 & 11
○ RUNS 23 & 26
URANIUM
ALUMINUM
COOLANT
GRAPHITE
CELL BOUNDARY
CHANGE OF SCALE

Figure 24. Effect of coolant along R radial

Runs made using medium foils (large foils were used in positions R4, R5 and R6 on run 31)

Run no.	Coolant	Region	Foil orientation	Spacing
12	None	graphite	vertical	2
16	None	fuel assembly	radial	normal
29	Water	graphite	vertical	2
31	Water	fuel assembly	radial	normal

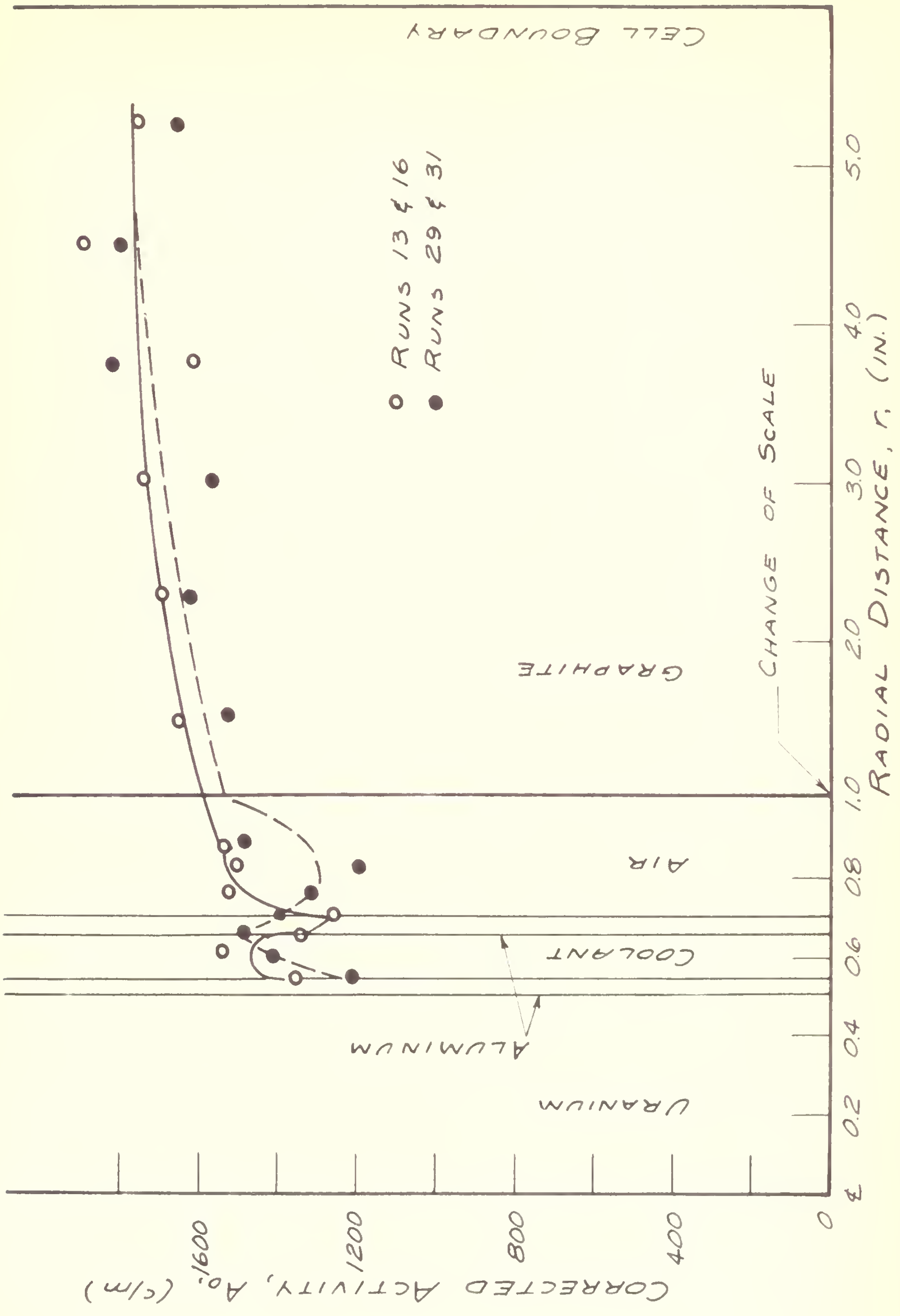
CELL BOUNDARY
○ RUNS 13 & 16
● RUNS 29 & 31
GRAPHITE
AIR
COOLANT
ALUMINUM
URANIUM
CHANGE OF SCALE
RADIAL DISTANCE, r, (IN.)
℄
0.2
0.4
0.6
0.8
1.0
2.0
3.0
4.0
5.0
CORRECTED ACTIVITY, A₀, (c/m)
0
400
800
1200
1600

when the average of the readings taken on the three radials was plotted as shown in Figure 25. There is seen a pattern that is fairly consistent with that predicted theoretically. That is, for the wet runs there is an increase in the thermal neutron flux across the water annulus, whereas for the dry runs the flux across the air annulus remains about constant. On the P and R radials it was noted that on the dry runs there was a rather sharp increase in flux (about 10 per cent) in the air hole beyond the process tube, whereas on the wet runs there was little if any increase in thermal neutron flux across this air space.

Figures 26 and 27 show results of runs which were made with and without coolant with foils in the fuel assembly close packed and foils in the graphite at spacing 1. There was considerably less scatter in the experimental data of Figures 26 and 27 than there was in Figures 22 and 24. This was probably due in part to the fact that for the close packed runs with spacing 1 in the graphite all of the foils were irradiated simultaneously in the same flux field. For spacing 2 and 3 there were two or three irradiations required to complete a survey along a radial. Since the foils were located differently for each irradiation, the flux field was shaped differently for each irradiation.

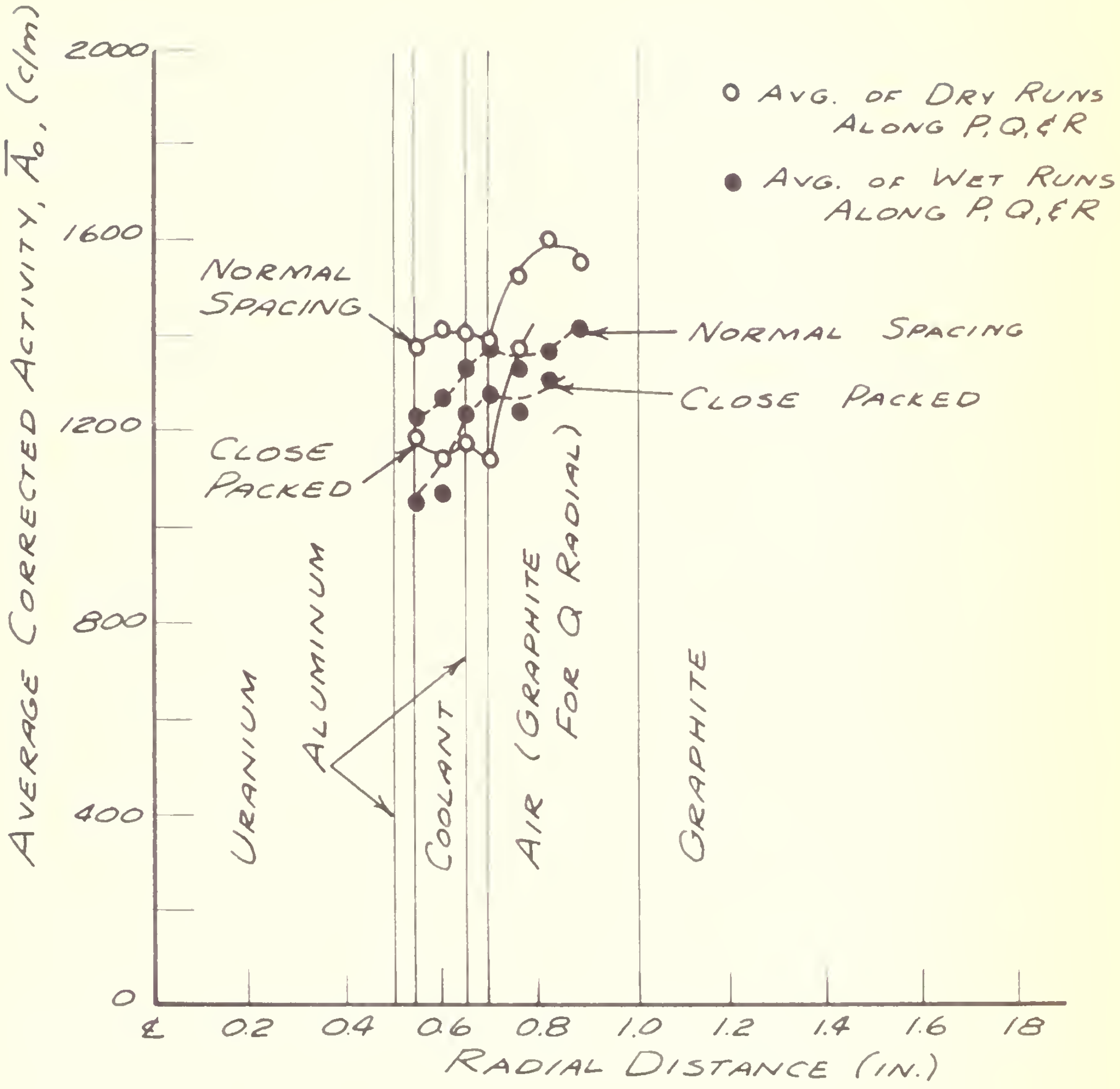

Figure 25. Average flux in fuel assembly

Figure 26. Effect of coolant along P radial with foils close packed in fuel assembly and at spacing 1 in the graphite

Run no.	Coolant
4	None
19	Water

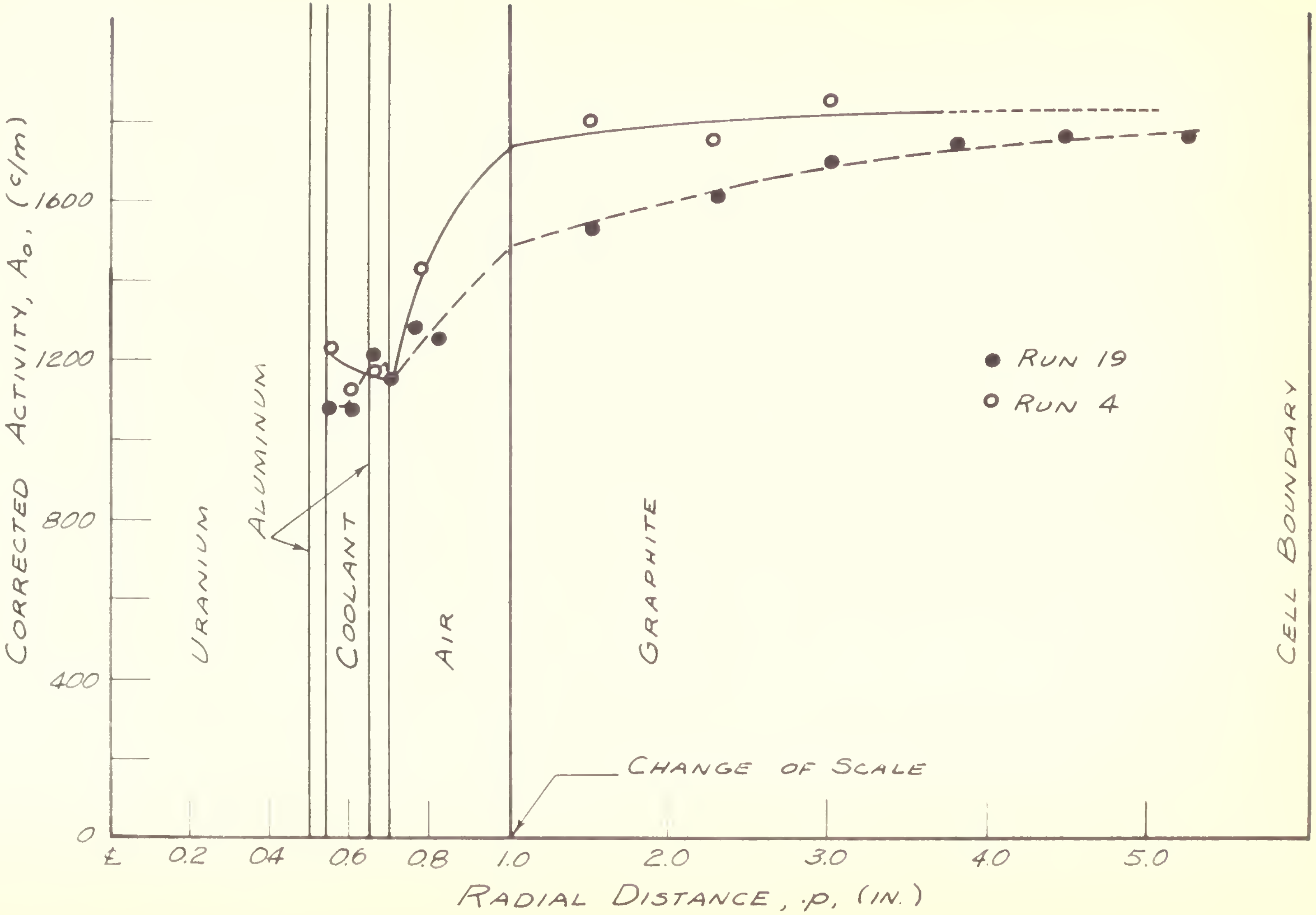
CORRECTED ACTIVITY, A_o, (c/m)
0
400
800
1200
1600
℄
0.2
0.4
0.6
0.8
1.0
2.0
3.0
4.0
5.0
RADIAL DISTANCE, ρ, (IN.)
URANIUM
ALUMINUM
COOLANT
AIR
GRAPHITE
CELL BOUNDARY
CHANGE OF SCALE
● RUN 19
○ RUN 4

Figure 27. Effect of coolant along R radial with foils close packed in fuel assembly and at spacing 1 in the graphite

Run no.	Coolant
15	None
30	Water

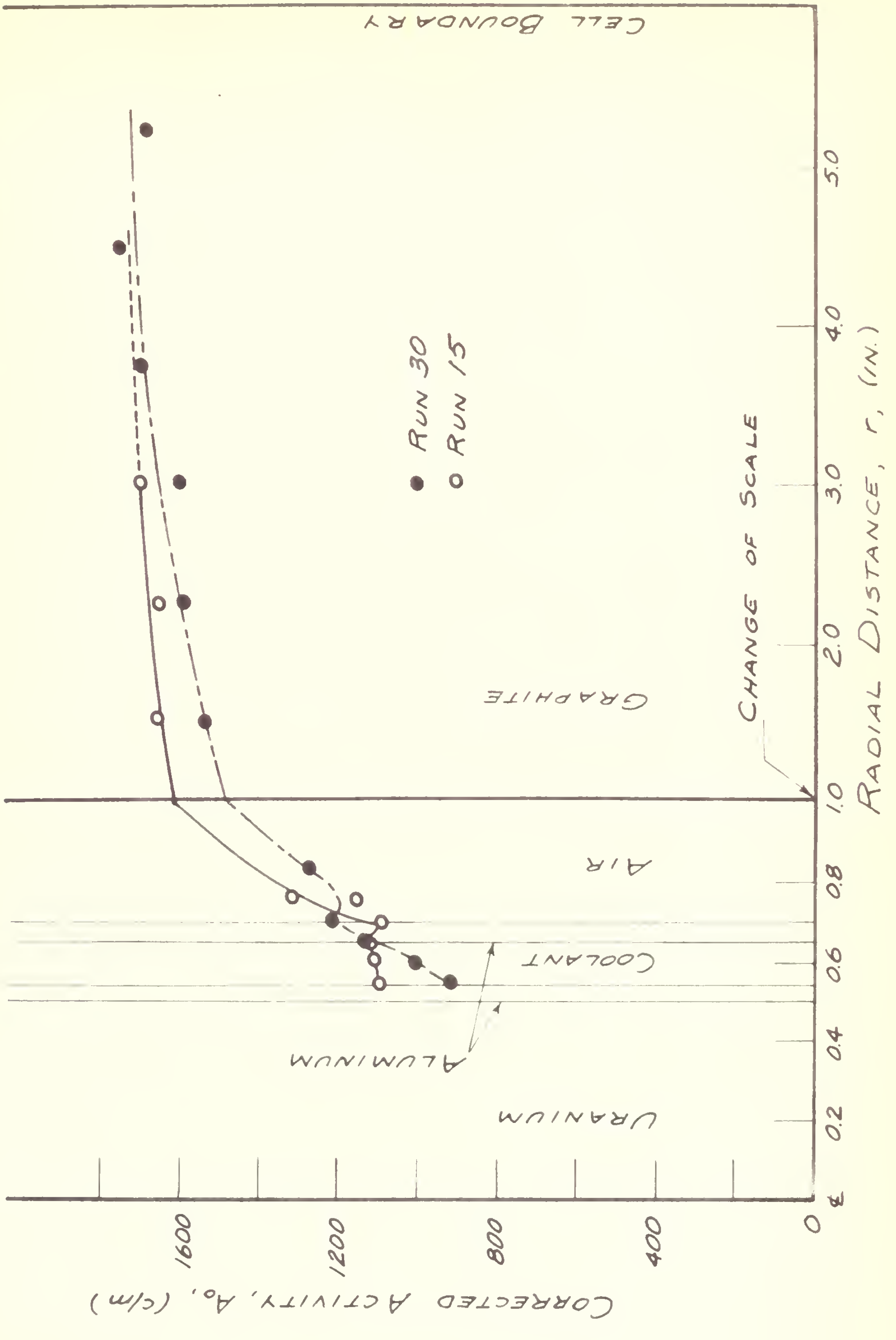
Cell Boundary
Graphite
Air
Coolant
Aluminum
Uranium
Change of Scale
● Run 30
○ Run 15
Radial Distance, r, (in.)
℄
0.2
0.4
0.6
0.8
1.0
2.0
3.0
4.0
5.0
Corrected Activity, A_o, (c/m)
0
400
800
1200
1600

F. Cadmium Ratio

Cadmium ratios were determined along the Q and R radials with coolant and are plotted in Figure 28. Along both radials the cadmium ratio increased with distance from the uranium. The increase along the Q radial was about 10 per cent at the unit cell boundary and along the R radial the ratio increased about 17 per cent at the cell boundary over what it was in the fuel assembly.

G. Comparison of Flux in Unit Cell With Overall Flux in the Assembly

Table 7 lists the results of the horizontal pile surveys taken at y = -10 in. and z = 30 in. with and without coolant. These surveys were taken using the large (1 in. by 1½ in.) aluminum backed indium foils. Plots of the horizontal pile surveys with and without coolant appear in Figure 29. Unit cell surveys along the R radial obtained with medium foils at spacing 2 are also plotted on Figure 29 to show the relationship of the unit cell flux distribution to the overall assembly flux distribution. The activities per gram obtained with the smaller unit cell foils were approximately 1.77 times larger than those obtained using the large (1 in. by 1½ in.) pile survey foils. The unit cell activities were divided by this factor of 1.77, and this reduced unit cell foil activity

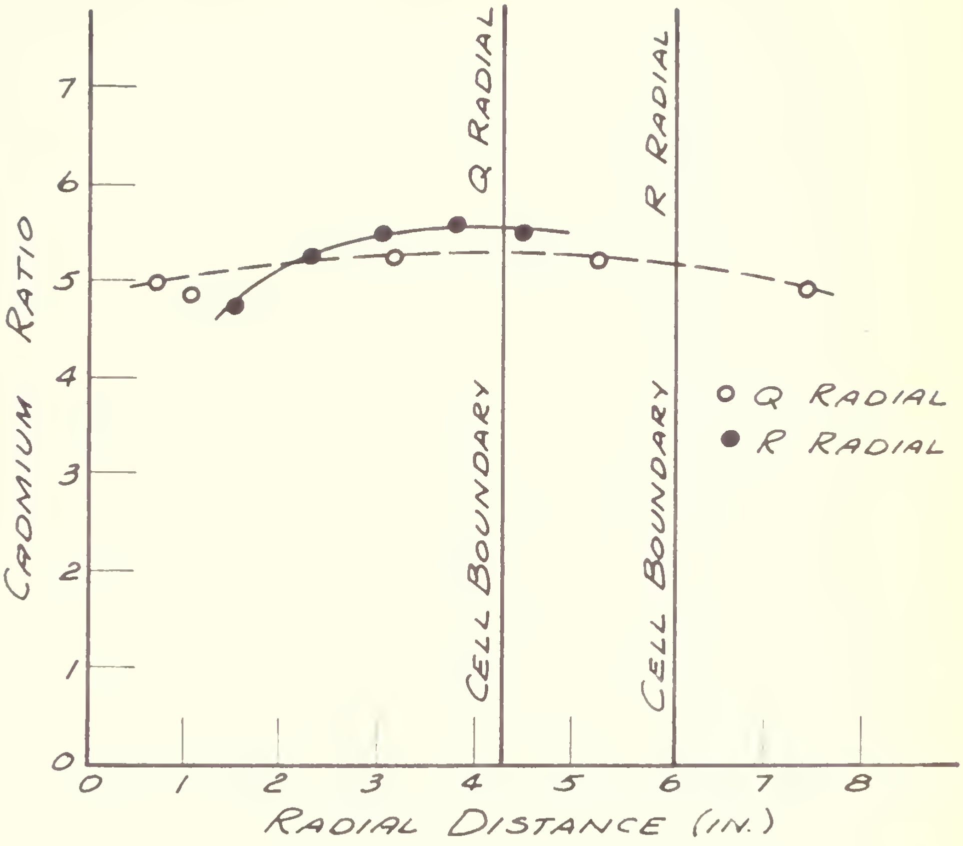

Figure 28. Cadmium ratios along Q and R radials (with coolant)

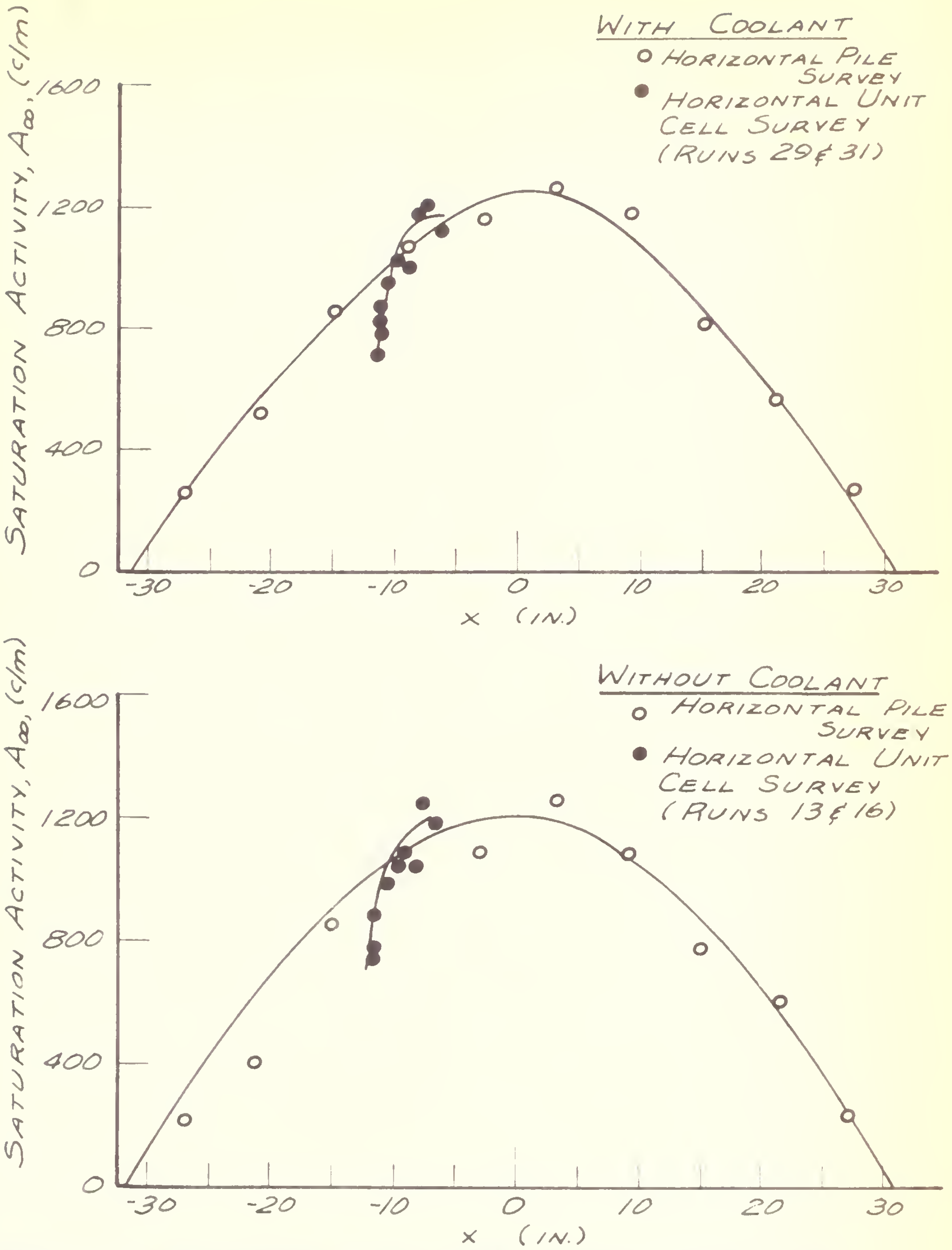

Figure 29. Horizontal flux surveys at y = -10 in. and z = 30 in.

was plotted on Figure 29.

Normalized saturation activities in the unit cell along the P radial using medium foils at spacing 2 with and without coolant were plotted on Figures 4 and 5 respectively to compare the vertical flux distribution in the unit cell with that in the pile. Since the overall vertical pile survey was taken at $x = -3$ in. and the vertical unit cell survey was taken at $x = -10$ in., there were no common points in the two surveys by which one set of data could be converted to the other. It was assumed that the ratio of activities would be the same as it was for the horizontal surveys. Thus the unit cell activities plotted in Figures 4 and 5 are the actual saturation activities reduced by the factor of 1.77 and corrected for the cosine distribution in the pile. The corrected vertical flux survey in the unit cell matched the vertical pile survey in the region remote from the fuel assembly.

VIII. DISCUSSION OF RESULTS

A. Techniques for Measuring Flux Distribution in a Unit Cell

In making any physical measurement great care must be taken not to influence the quantity measured by the technique of measuring. This is especially true in the case of neutron flux measurement by the foil activation method. It is impossible to avoid altering the flux field when using the activation method, but it is possible to keep these alterations as small as possible. Space must be made available for placing the indium foils, and the foils must be large enough so that their induced activities after irradiation in the neutron flux are detectable and meaningful.

In order to obtain reproducible results it is of primary importance to obtain sufficiently good counting statistics. Due to the smallness of the indium foils, the low neutron flux, and the 54 minute half life of indium, the allowed counting time is limited. Use of gold foil with its longer half life would help solve this problem, but would require longer irradiation times. If several foils were to be counted it was found best to use short counts and count through all the foils two or more times and average these

rather than take single long counts. Although averaging the saturation activities obtained from several short counts did not appreciably improve the counting statistics it did help a great deal in reducing the scatter of the experimental data. This was probably due to the fact that averaging tended to reduce the variations in counting geometry from one foil to another. The counting geometry of the foils must of course be kept constant as well as the geometry of the foil while it is being irradiated. This was probably the main reason why the L-shaped foils gave such erratic results on run 10. In bending the foils into the 90° angle some were undoubtedly bent slightly different than others and thus had different irradiation geometry. Furthermore when these bent foils were counted it was difficult to flatten them out under the counter and this introduced variations in counting geometry. By irradiating the foils flat, either horizontally or vertically, the above difficulties were eliminated.

Foil size, spacing, loading and counting time should be determined by the type of results desired and the time available to collect the data. If quantitative results on the unit cell are desired, the smallest foils possible should be used, and they should be irradiated in the unit cell one at a time. The minimum size of the foil would depend on the flux level. For the flux encountered in these experiments it was found that the minimum usable size of 0.003-in. indium

foil was ¼ in. by ¼ in. If only qualitative results are desired, for example, if it is desired to determine only the pattern of the flux distribution, the foils placed in the unit cell may be larger both in size and in number. Even placing the foils close packed in the fuel assembly and placing the foils at spacing 1 in the graphite did not appear to greatly distort the flux distribution in the unit cell. Although the general flux level was depressed by close packing the foils in the fuel assembly, the general shape of the flux distribution was not greatly altered as is shown in Figure 25.

Using the activation method is a time consuming process when using small foils in a low neutron flux due to the fact that the foils must be irradiated about 6 hours between each run. It is therefore most advantageous to read as many foils as possible per irradiation. With the size foils used it was found that the maximum number of foils it was practical to read at one time was eight. By using two or more counters simultaneously it would be possible to reduce the time required for counting per irradiation and also the number of irradiations per run.

B. The Flux Distribution in a Unit Cell

The matching of the flux distribution curves along the

P, Q and R radials as was seen in Figures 18 and 19 would seem to verify the validity of the f_x and f_z correction factors which were questioned by Clayton (2, p. 33). At least they seem to be valid within the limits of accuracy of this investigation.

The general effect of water in the coolant annulus of the fuel assembly was to depress the flux in the fuel assembly and in the surrounding graphite. With the exception of the flux pattern shown in Figure 23 it appeared that there was very little if any depression of flux in the region near the unit cell boundary. Hence, horizontal and vertical flux surveys made across the assembly with the survey foils located near the unit cell boundaries would not detect any variation in the flux distribution due to the addition of coolant. The survey foil positions in the subcritical assembly used in this investigation were located half way between the centers and the boundaries of the unit cells so that the depression of flux due to the coolant was hardly detectable. Although not very pronounced the moderating effect of the water was apparent from the experimental data plotted in Figures 23 through 26. With improved statistics and refined counting procedures it should be possible to measure quite accurately the effect of coolant on the flux distribution in the fuel assembly.

The high foil activities obtained in the unit cell as

compared with those activities obtained when making horizontal flux surveys across the entire assembly were probably due mainly to the counting geometry. The geometry factor for the unit cell foils approached 50 per cent since these foils were completely covered by the window of the counting tube which was 1 1/8 in. in diameter. However the large foils used in making the overall pile surveys extended out beyond the counter window. This would cause the activity per gram for the small foils to be higher than for the large foils.

The unit cell foil activities which are plotted on Figure 29 indicate that the flux distribution across the assembly has large deviations from the cosine distribution due to the depressions in the vicinity of the fuel assemblies. This points up again the importance of foil placement when making flux surveys. Three different horizontal flux distributions would be obtained across the assembly depending on whether the foils were placed in the empty holes, in the survey slots or in the holes loaded with fuel elements. These are shown as curves A, B and C respectively in Figure 30. The actual flux distribution would be shaped like curve D with depressions at the fuel elements and peaks at the cell boundaries. The depressions in the region of the fuel assemblies are probably not as pronounced as the experimental data indicates because the presence of the indium was partly responsible for the lowered flux.

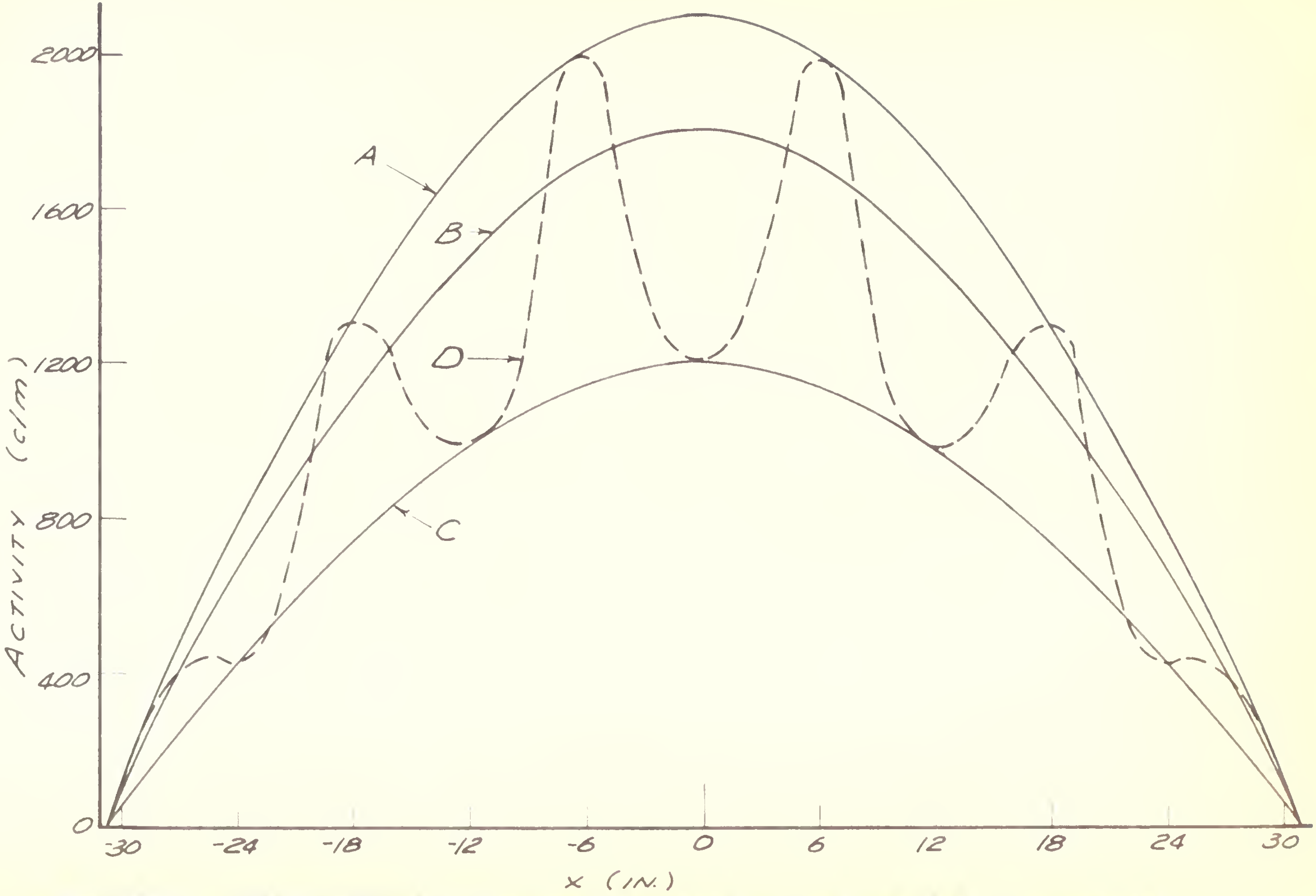

Figure 30. Hypothetical horizontal surveys for various foil placements

Unit cell foil activities along the P radial were plotted on Figures 4 and 5 simply to show that the vertical flux distribution also deviates considerably from the theoretical exponential drop. It is apparent that when irradiating foils for the purpose of determining the buckling, it is important that the foils be irradiated at the same relative position in each unit cell. The validity of the position correction factor, f_x, would again appear to be verified from the fact that when it was applied to the unit cell survey data, the corrected data matched the pile survey data very closely in the region away from the fuel assembly.

The shapes of the cadmium ratio curves in Figure 28 show that the fast neutron flux in the region near the fuel assembly is higher than in the region near the unit cell boundary. The cadmium ratios obtained along the Q radial indicate that the fast neutron flux is symmetrical with respect to the center of the fuel slug. Since a low cadmium ratio indicates a relatively higher fast neutron flux, it is apparent that the fast flux becomes maximum in the fuel assembly, drops off as the cell boundary is approached, and increases again as the slug in the adjacent unit cell is approached. The higher cadmium ratio at the cell boundary along the R radial as compared to that along the Q radial was due to the factthat the cell center-to-boundary distance was greater along the R radial, and hence there were fewer fast

neutrons remaining at the cell boundary in the R direction than there were in the Q direction.

C. Comparison of Experimental Results with Theory

The theoretical flux distribution in the unit cell of a simple two-region fuel-moderator system is shown as curve A in Figures 31 and 32. Curves B and C are the theoretical flux distributions in a multiregion system with and without coolant respectively. Since the experimental results indicated there was very little depression of flux in the region near the unit cell boundary due to the water coolant, the theoretical curves were normalized to the cell boundary flux.

Results of flux surveys along the P and R radials for both wet and dry runs are plotted on Figures 31 and 32, where the experimental data was normalized to the average cell boundary flux. Two-region theory is seen to agree quite well with the experimental data. However a curve through the experimental points would have less slope than that predicted by Murray. Multiregion theory both with and without water coolant appears to give high values for the flux in the graphite but the shape of the curve appears to agree closely with the experimental data. In multiregion theory the variation of flux across the cladding, coolant and process tubes was assumed to be linear, and the flux across air gaps was

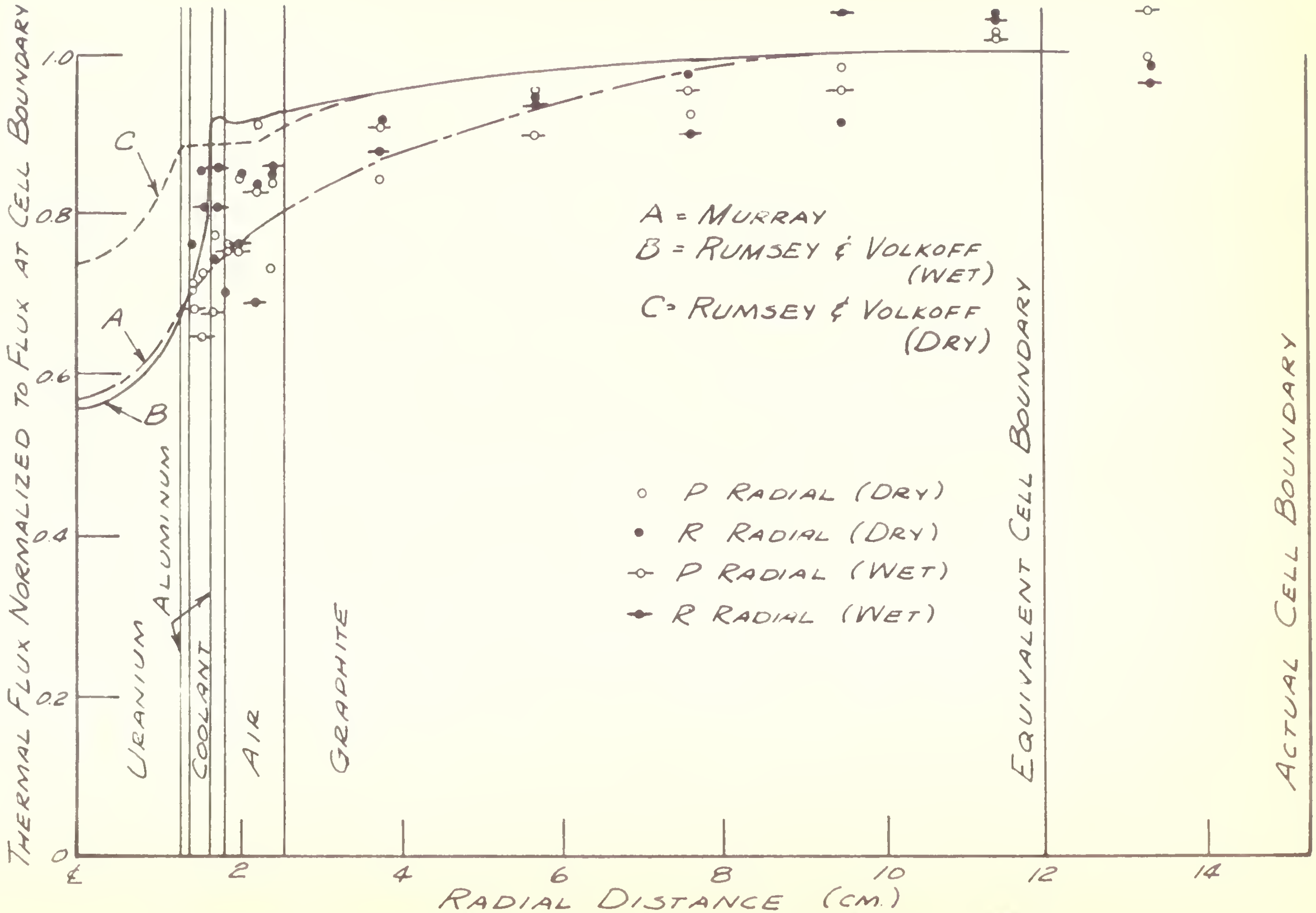

Figure 31. Comparison of experimental data with theory

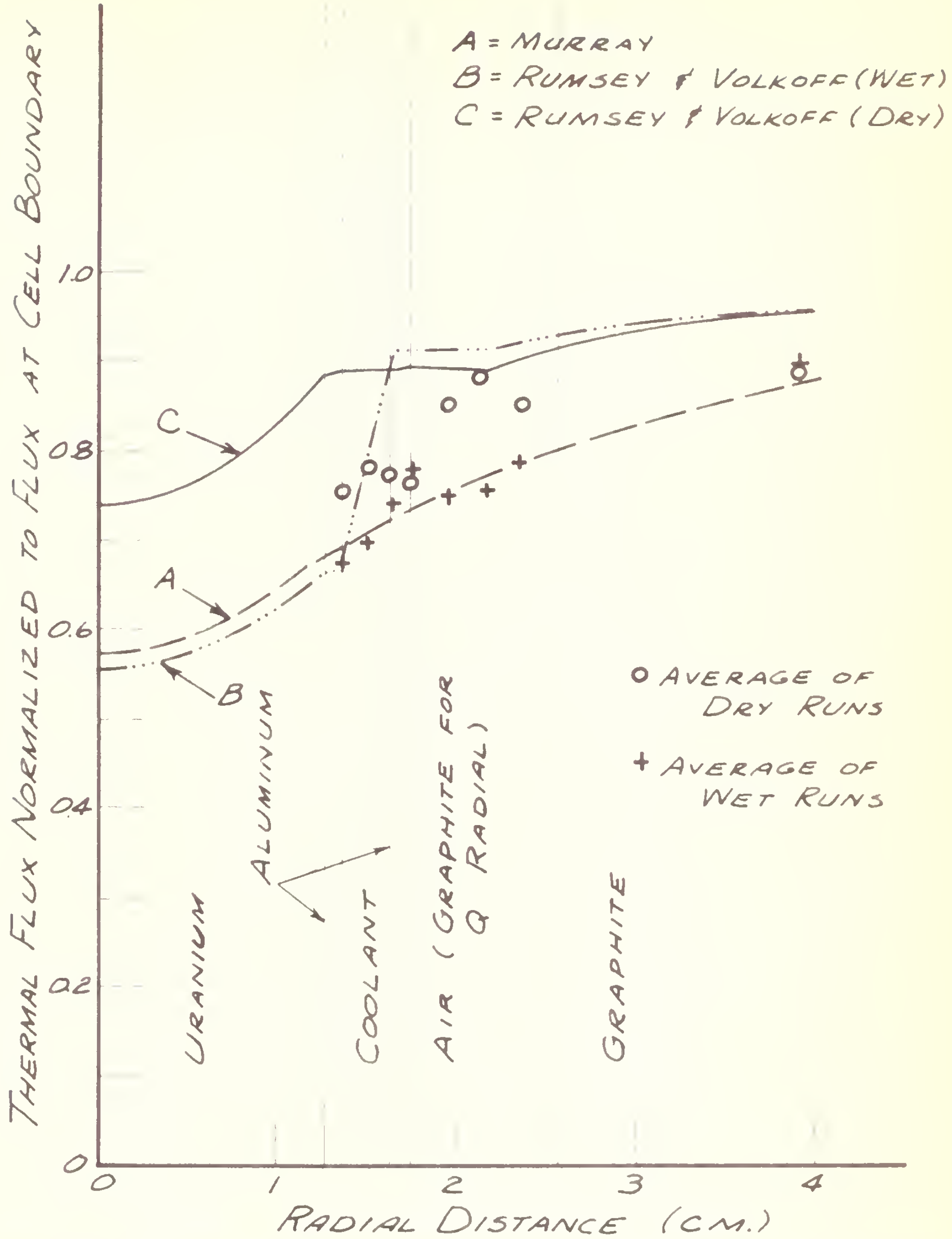

Figure 32. Comparison of experimental data with theory

assumed to be constant. These assumptions appear to be valid except for the water coolant. The theoretical decrease in flux across the water annulus was about twice as large as that observed. This discrepancy was probably due to the fact that the moderating effect of the water was ignored in calculating the theoretical curves. Although the theory of Rumsey and Volkoff provides for the moderating effect of the water in determining the thermal utilization of the lattice, it does not provide for the inclusion of this effect in calculating the flux distribution.

IX. CONCLUSIONS

The activation method is quite adaptable to the measurement of neutron flux in the unit cell. By reducing the statistical deviation of the foil activities it should be possible to determine accurately the flux distribution. For more exact calculations it would also be necessary to correct foil activities for the fast neutron flux which is present and measured along with the thermal flux.

The flux distribution predicted by two-region theory is in very close agreement with the observed distribution. Murray's assumption that any poisons that are tolerable do not appreciably disturb the basic fuel-moderator flux distribution appears to be reasonably valid, although these poisons do flatten out the flux distribution in the graphite. Multi-region theory appears to predict a flux level in the moderator which is generally higher than was observed. It also gave a larger flux depression across the water coolant, because the moderating effect of the water was ignored.

X. SUGGESTIONS FOR FURTHER STUDY

Further investigation of the flux distribution in the unit cell of the subcritical assembly could be carried out by varying certain other parameters, such as coolant, lattice size and slug size. One could also examine other unit cells either adjacent to the one examined herein or in another region of the assembly. On any further work the flux surveys might be continued into the fuel element itself.

The apparent rise in the flux in the air gap beyond the process tube along the F and H radials presents an interesting phenomenon which could be further investigated. The flux pattern in this region is apparently dependent upon the flux pattern in the coolant annulus, however the statistical deviation of the experimental data of this investigation prohibits making any definite conclusion along these lines.

Another subject for investigation could be the theoretical development of the flux distribution in the unit cell. As was previously pointed out, the theory of Rumsey and Volkoff was primarily aimed at a more refined prediction of the thermal utilization rather than an exact solution of the point-to-point flux distribution. By extending diffusion theory to the multiregion system it would be possible to

obtain the theoretical flux distribution in each region. Such treatment would be particularly adaptable to predicting the flux distribution across a moderating region, such as the water filled coolant annulus.

XI. LITERATURE CITED

1. Akademiia nauk, SSSR. Matematicheskii institut imeni V. A. Steklova. Tablitsy znachenii funktsii Besselia ot mnimogo argumenta. Moskva, Izdatelyestvo Akademii nauk SSSR, 1950.

2. Clayton, E. D. Exponential pile measurements in graphite-uranium lattices. U.S. Atomic Energy Commission. Report AECD-3677 (Atomic Energy Commission Declassified) Washington, D. C., Office of Technical Services, Department of Commerce. June 1, 1954.

3. Cohen, E. R. The role of exponential experiments in reactor design. Nuclear engineering--Part II. American Institute of Chemical Engineers. Chemical Engineering Progress Symposium Series 50, no. 12: 72-81. 1954.

4. Feld, Bernard T. The application and experimental basis of pile theory. In Goodman, Clark, ed. Introduction to pile theory. 2nd ed. pp. 187-230. Cambridge, Mass., Addison-Wesley Press, Inc. 1952.

5. Gast, Paul F. Normal uranium, graphite moderated reactors: a comparison of theory and experiment--water cooled lattices. International Conference on the Peaceful Uses of Atomic Energy Proc. 5: 288-294. 1956.

6. Glasstone, Samuel and Edlund, Milton C. The elements of nuclear reactor theory. Princeton, N. J., D. Van Nostrand Co., Inc. 1952.

7. Guggenheim, E. A. and Pryce, M. H. L. Uranium-graphite lattices. Nucleonics 11, no. 2: 50-60. February 1953.

8. Hoganson, John Henry. Operating characteristics of a uranium graphite subcritical assembly with coolant simulation. Unpublished M. S. Thesis. Ames, Iowa, Iowa State College Library. 1957.

9. Hummel, Virginia and Hamermesh, Bernard. Flux depression in the neighborhood of a foil. In Wattenburg, A. and McCorkle, W. H., eds. Experimental Nuclear Physics Division and Theoretical Nuclear Physics Division Report for January, February, and March 1950. p. 62. U. S. Atomic Energy Commission. Report ANL-4437 (Argonne National Laboratory) Washington, D. C., Office of Technical Services, Department of Commerce. April 5, 1950.

10. Murray, Raymond L. Nuclear reactor physics. Englewood Cliffs, N. J., Prentice-Hall, Inc. 1957.

11. Richey, C. R. Thermal utilization and lattice diffusion length in graphite-uranium lattices from exponential pile measurements. U. S. Atomic Energy Commission. Report AECD-3675 (Atomic Energy Commission Declassified) Washington, D. C., Office of Technical Services, Department of Commerce. April 1, 1954.

12. Rumsey, V. H. and Volkoff, G. M. Diffusion theory expressions for the thermal utilization factor in cells with slab, cylindrical and spherical geometry. Atomic Energy of Canada Limited. MT-221 (National Research Council of Canada. Montreal Laboratory.) May 30, 1946. (Original not available for examination; cited and partially reproduced in Clayton, E. D. and Richey, C. R. Correlation of exponential pile lattice measurements with theory. pp. 17-22. U.S. Atomic Energy Commission. Report HW-25038. (Hanford Atomic Products Operation, Richland, Washington) Washington, D. C., Office of Technical Services, Department of Commerce. February 8, 1955.)

XII. ACKNOWLEDGMENTS

I wish to express my sincere thanks to Dr. Robert L. Uhrig for the initial suggestion of this thesis problem and for his generous assistance throughout the course of the work. Special thanks are also due to Dr. Glenn Murphy for his encouragement and assistance during my stay at Iowa State College.

This thesis culminates three years of postgraduate instruction in Aeronautical Engineering (Nuclear Propulsion), and I wish to express my deep appreciation to the United States Navy and in particular to the United States Naval Postgraduate School for the opportunity of receiving this advanced education.

XIII. APPENDIX

Table 8. Dimensions and material constants for the unit cell

Dimensions			
r_u	, uranium rod radius	1.270	cm
t_{al}	, thickness of aluminum cladding	0.102	cm
t_w	, effective thickness of water annulus	0.273	cm
t_p	, effective thickness of process tube	0.102	cm
t_{air}	, effective thickness of air annulus	0.455	cm
r_1	, equivalent inner radius of graphite	2.20	cm
r_2	, equivalent outer radius of graphite	11.94	cm
Volume per slug			
V_u	, uranium	103.0	cm^3
V_{al}	, slug can and cap	23.0	cm^3
V_w	, water	55.7	cm^3
V_p	, process tube	22.6	cm^3
V_g	, graphite	9250	cm^3
Absorption cross sections			
Σ_{al}	, aluminum	0.01323	cm^{-1}
Σ_u	, uranium	0.324	cm^{-1}
Σ_g	, graphite	0.00036	cm^{-1}
Σ_w	, water	0.017	cm^{-1}
Inverse diffusion lengths			
κ_u	, uranium	0.675	cm^{-1}
κ_g	, graphite	0.01992	cm^{-1}
κ_w	, water	0.3472	cm^{-1}
κ_{al}	, aluminum	0.0495	cm^{-1}

thesH404
Flux distribution in a unit call of a ur
3 2768 002 08643 1
DUDLEY KNOX LIBRARY